Hyperglycemia-induced Changes in ZIP7 and ZnT7 Expression Cause Zn^{2+} Release from the Sarco(endo)plasmic Reticulum and Mediate ER-stress in the Heart

Erkan Tuncay[1], Verda C. Bitirim[1], Aysegul Durak[1], Gaelle R. J. Carrat[2], Kathryn Taylor[3], Guy A. Rutter[2*] and Belma Turan[1*†]

[1]Department of Biophysics, Ankara University, Faculty of Medicine, Ankara, Turkey; [2]Section of Cell Biology and Functional Genomics, Division of Diabetes Endocrinology and Metabolism, Department of Medicine, Imperial College London, London, UK, and [3]School of Pharmacy and Pharmaceutical Sciences, College of Biomedical and Life Sciences, Cardiff University, Cardiff, UK

Running title: Hyperglycemia and zinc-transporters in mammalian heart

Key words: Zinc transporters, cytosolic zinc, diabetic cardiomyopathy, heart, ER stress, sarco(endo)plasmic reticulum, FRET, Protein kinase-2.

[*]equal senior scientists.

[*†]**Correspondence:** Belma Turan, PhD ([†]lead)
Department of Biophysics, Faculty of Medicine, Ankara University, Ankara, Turkey.
Tel: +90 312 5958186
Fax: +90 312 3106370
Email: belma.turan@medicine.ankara.edu.tr

or

[*]
 Guy A. Rutter PhD
Section of Cell Biology and Functional Genomics, Division of Diabetes Endocrinology and Metabolism, Department of Medicine, Imperial College London, London, UK,
Tel: +44 20 759 43340
Fax: +44 20 759 43351
Email: g.rutter@imperial.ac.uk

Abstract

Cellular free Zn^{2+}-changes, including those in the sarco(endo)plasmic reticulum [S(E)R], are primarily coordinated by Zn^{2+} transporters. The role of these in the heart is not well established. To investigate the hypotheses that ZIP7 and ZnT7 transport Zn^{2+} in opposing directions across the S(E)R membrane in cardiomyocytes and that changes in the expression of these transporters play an important role in development of ER-stress during hyperglycemia. The subcellular localization of ZIP7 and ZnT7 was determined in rat cardiomyocytes by immunofluorescence imaging and confirmed by Western (immune-) blot analysis of isolated S(E)R preparations. ZIP7 mRNA and protein levels were increased in ventricular cardiomyocytes from diabetic rats or high glucose-treated H9c2 cells whilst ZnT7 expression was lowered under these conditions. The above changes were associated with ER stress. Assessed using recombinant-targeted eCALWY Zn^{2+} probes, hyperglycemia induced a marked redistribution of cellular free Zn^{2+}, increasing cytosolic free Zn^{2+} and lowering free Zn^{2+} in the S(E)R. Silencing of ZIP7 prevented these changes. High glucose also increased expression of protein kinase 2 consistent with a role of the latter kinase in controlling ZIP7 activity. Opposing changes in the expression of ZIP7 and ZnT7 are likely to contribute to a redistribution of intracardiomyocyte Zn^{2+} in hyperglycemia and to diabetes-induced cardiac dysfunction. These data provide novel and important insights into how cellular free Zn^{2+} re-distribution, resulting from altered ZIP7 and ZnT7 activity in the hyperglycemic heart, can contribute to cardiac dysfunction in diabetes. In summary, these findings may provide new targets against diabetes-induced cardiac dysfunction for the new therapeutic strategies.

Introduction

Diabetes mellitus (both Type 1 and Type 2) is an important risk factor for the development of cardiovascular complications, which is due, in large part, to defective cytosolic Ca^{2+} signaling (1-3) . Previously, we have shown that Zn^{2+} release during cardiac cycle (4) results mostly in a cytosolic free Zn^{2+} increase, further triggering higher production of pro-oxidant species and leading to oxidative damage (5). Conversely, it has also been shown that either acute or chronic oxidant exposure induces marked increases in cytosolic free Zn^{2+} in cardiomyocytes (6) while either acute or chronic hyperglycemia causes oxidative stress and increased levels of cytosolic free Zn^{2+}, underling electrical and mechanical dysfunction in the heart (7; 8). Similar to Ca^{2+}, Zn^{2+} is essential for several cellular functions in mammalian heart, including cell growth and differentiation (9), serving up as an important secondary messenger (10).

Zn^{2+} deficiency in mammals (11) can increase the risk of development of many complications. Conversely, excess Zn^{2+} can be detrimental to cellular health, particularly that of cardiomyocytes (4; 6; 7; 9). Free cytosolic Zn^{2+} has an important role in excitation-contraction coupling in cardiomyocytes by shaping Ca^{2+} dynamics (4; 5; 12). The free cytoplasmic Zn^{2+} concentration in cardiomyocytes is calculated to be less than 1 nM under physiological conditions, while it is ~5-fold higher in sarco(endo)plasmic reticulum [S(E)R] by using Frster resonance energy transfer (FRET)-based recombinant-targeted Zn^{2+} probes (13). Elevated cytosolic free Zn^{2+} appears to contribute to deleterious changes in many signaling pathways, similar to those observed in hyperglycemia-challenged cardiac cells (4-7; 14).

Cellular Zn^{2+} fluxes are achieved and controlled by families of Zn^{2+}-transporters (ZnT) and importers (ZIP) (15; 16). The cellular distributions and functions of these transporters are not yet well clarified in mammalian cardiomyocytes. As reviewed recently (16), the ZIP family increases the cytosolic free Zn^{2+} level by promoting extracellular uptake or release of these

ions from subcellular organelles, whereas ZnT family members function as counter regulators via efflux of cytosolic Zn^{2+} (16). Many proteins use Zn^{2+} as an important cofactor and the Zn^{2+}-selective ion channel ZIP7 has important role for releasing Zn^{2+} from the ER and Zn^{2+}-associated induction of unfolded protein response in yeast (17). Similarly, ZIP7 is believed to be localized to the Golgi apparatus in Chinese Hamster Ovary cells, where it allows Zn^{2+} release from the Golgi lumen into the cytosol (18). ZIP7 facilitates the release of Zn^{2+} from the ER (19) and behaves as a critical component in the sub-cellular re-distribution of Zn^{2+} in other systems (20). Additionally, it has been hypothesized that protein kinase-2 (CK2) triggers cytosolic Zn^{2+} signaling pathways by phosphorylating ZIP7 (21). Recent studies have also highlighted the important contribution of ZIP7 to Zn^{2+} homeostasis in mammalian cells, particularly under pathological conditions (22-24).

Of note, the expression profiles of the Zn^{2+} transporters vary markedly and are dependent on tissue type and health or disease state as well. Although early and recent studies have shown the presence of the weakly expressed Zn^{2+}-transporters ZIP7 and ZnT7 in mammalian heart (25; 26), their subcellular localizations and functional roles under physiological and pathological conditions are not yet known. In that regard, recent studies have suggested that either increase or inhibition of either ZIP7 or ZnT7 might contribute to cellular dysfunction, including defective insulin-mediated signaling pathways under high glucose (27) or altered insulin secretion from the pancreatic β cell (28). Polymorphisms in the genes encoding Zn^{2+}-transporters play also play important roles in a number of inherited human diseases, including diabetes mellitus (29-31).

ER stress is one of the underlying mechanisms of cardiac dysfunction including diabetic cardiomyopathy (32-35) and there is relationship between if S(E)R function cytosolic free Zn^{2+} level in diabetic rat cardiomyocytes (34; 36). In particular, the latter studies identified a close association between oxidative stress, cytosolic free Zn^{2+} increases, ER-stress and cardiac

dysfunction in diabetes. Other experimental evidence suggests a requirement for Zn^{2+} for proper ER-function, with Zn^{2+} deficiency leading to induction of ER-stress (17; 37). In another direction, activation of an ER-stress response has also been observed when Zn^{2+} is decreased in the ER via hypoxia or hypoglycemia (17; 38). However, there are no clear data as to which Zn^{2+}-transporters play roles in controlling cytosolic free Zn^{2+} increases in cardiomyocytes during hyperglycemia.

It is therefore tempting to hypothesize that the disruption of a Zn^{2+} transporter-Zn^{2+} axis may contribute to deleterious changes in cardiomyocytes in diabetes. Here, we provide evidence for the existence of a Zn^{2+} transporter system comprising ZIP7 and ZnT7 which are localized to the S(E)R and transport Zn^{2+} in opposing directions. If such a system were perturbed during hyperglycemia, depleting S(E)R Zn^{2+}, this may in turn lead to ER-stress. In this study, we aimed firstly to clarified the subcellular localizations of ZIP7 and ZnT7 in cardiomyocytes and then to explore their functional roles on Zn^{2+} homeostasis. Additionally, we tested the role of cytosolic free Zn^{2+} re-distribution and the development of ER-stress in hyperglycemic conditions, and the role in this of process of CK2. Our results provide evidence of a key role for ZIP7 and ZnT7 which are perturbed by hyperglycemia and can contribute to the development of cardiac dysfunction via induction of ER-stress in diabetic subjects.

Research Design and Methods

Rats and Diabetes Induction

Our study was approved by the local experimental animal ethic committee of Ankara University (115-449). We used 3-month-old male Wistar rats and diabetes (mimic of Type 1 diabetes) was induced by a single injection of streptozotocin (STZ, 50 mg/kg dissolved in 0.1 M citrate buffer at pH 4.5; intraperitoneal; Sigma-Aldrich), as described previously (3). The second group of rats, kept as controls (CON group), were injected with citrate-buffered saline. A week after the, blood glucose levels were measured and rats with blood glucose levels at

least 3-fold higher than the pre-injection levels were used as diabetic group (DM group).

Cardiomyocyte Isolation

Left ventricular myocytes were isolated from fresh tissue, as described previously (6). Shortly, rats were anaesthetized with sodium pentobarbital (30 mg/kg body weight, intraperitoneal), and the hearts were removed and cannulated on a Langendorff apparatus leaving perfused retrogradely through the coronary arteries with a Ca^{2+}-free solution. Hearts were perfused to clean out for 5-6 minutes, followed by perfusion with the same solution containing 1 mg/mL collagenase (Collagenase Type 2, Worthington, USA) for 30-35 minutes. In every isolation procedure, the percentage of viable cells was more than 80% in either group. Only Ca^{2+} tolerant cells were used incubated in a 1 mmol/L Ca^{2+} containing solution.

Cell Culture

The left ventricle of the embryonic rat heart tissue-derived H9c2 cardiac myoblast cell line was purchased from American Type Culture Collection (Manassas, VA). Cells were cultured in Dulbecco's modified Eagle's medium, supplemented with 10% fetal bovine serum and 100 units penicillin-streptomycin at 37°C in a humidified 5% CO_2-95%. Cells were grown at a density of about 10^5 cells/cm^2 in DMEM modified by using 5.5 mM glucose instead of high glucose and supplemented with 10% fetal calf serum, 50 U/mL penicillin-G and 50 μg/mL streptomycin in a humidified atmosphere of 95% air and 5% CO_2.

Imaging and Quantification of Cytosolic and Sarco(endo)plasmic Reticulum of Free Zn^{2+} Levels Using FRET-Based eCALWY Probes

Cytosolic and S(E)R free Zn^{2+} levels ($[Zn^{2+}]_{Cyt}$ and $[Zn^{2+}]_{ER}$, respectively) in H9c2 cells were measured by using eCALWY sensors (Cyt-eCALWY4 and ER-eCALWY6), delivered with plasmids expressing Cyt-eCALWY4 and ER-eCALWY6 and ratiometric measurements are performed as described previously (13). Briefly, Images were captured at 433 nm

monochromatic excitation wavelength (Polychrome IV, Till photonics) using an Olympus IX-70 wide-field microscope with a 40×/1.35NA oil immersion objective and a zyla sCMOS camera (Andor Technology) controlled by Micromanager software. Image analysis was performed with ImageJ software using a homemade macro and the fluorescence emission ratios were derived after subtracting background. The steady-state fluorescence intensity ratio citrine/cerulean (R) was measured, then maximum and minimum ratios were determined to calculate free Zn^{2+} level by using the following formula: $[Zn^{2+}]=K_d(R_{max}-R)/(R-R_{min})$. The maximum ratio ($R_{max}$) was obtained upon intracellular Zn^{2+} chelation with 50 μM heavy metal chelator N,N,N',N'-tetrakis(2-pyridylmethyl) ethylenediamine (TPEN, Sigma-Aldrich, USA) and the minimum ratio (R_{min}) was obtain upon Zn^{2+} saturation with 100 μM $ZnCl_2$ in the presence of an ionophore pyrithione (Pyr, 5 μM).

Sub-Cellular Localization of ZIP7 and ZnT7 in Cardiomyocytes Using Confocal Microscopy

Localization of the endogenous Zn^{2+} transporters, ZIP7 (Thermofisher, PA5-21072; 1:50) and ZnT7 (Santa Cruz, SC-160946; 1:50) in cardiomyocytes was determined by using anti-ZIP7 and anti-ZnT7 antibodies, respectively, using confocal microscopy (Zeiss LSM510). S(E)R localization was determined by transfection of H9c2 cells with dsRED-ER (red) plasmid for 24 hours. After fixation and permeabilization of H9c2 cells with 4% paraformaldehyde and 0.2% Triton-X100, respectively, they were incubated with either the ZIP7 or ZnT7 antibody to monitor the localization of ZIP7 and ZnT7 protein in the S(E)R. After overnight incubation of the cells, they were further incubated with appropriate secondary antibodies in the presence of 5% (w/v) BSA (Alexa Fluor 488 Donkey anti-Rabbit for ZIP7; 1:1000, Alexa Fluor 488 Donkey anti-Goat for ZnT7; 1:1000).

The Golgi apparatus was labeled using an Anti-GM130 antibody cis-Golgi Marker (Abcam; ab52649; 1:750). After fixation and permeabilization, H9c2 cells were incubated either with

anti-ZIP7, -ZnT7 or the Golgi marker GM130 antibody to demonstrate the localization of ZIP7 and ZnT7 protein in this compartment. Following overnight incubation, cells were further incubated with appropriate secondary antibodies (Alexa Fluor 488 Donkey anti-Rabbit for ZIP7; 1:1000 and Alexa Fluor 568 Goat anti-Mouse for GM130; 1:1000, Alexa Fluor 488 Donkey anti-Goat for ZnT7; 1:1000 and Alexa Fluor 647 Rabbit anti-Mouse for GM130; 1:1000) and were mounted with medium containing DAPI (blue). Images were deconvolved and analyzed for colocalization by using Huygens software and processed with ImageJ (https://svi.nl/HuygensProfessional).

Isolation of Sarco(endo)plasmic Reticulum from Rat Heart

Sarco(endo)plasmic reticulum, S(E)R fractionation of small trabeculae isolated from left ventricle of rat heart was performed by using an ER isolation kit (Sigma, E0100). Briefly, heart tissues were homogenized in isotonic extraction buffer and then centrifuged. The crude microsomal fraction was isolated from a post-mitochondrial fraction by using ultracentrifugation. For further purification and separation of RER (rough ER) and SER (smooth ER) from microsomes, self-generating density gradient procedure was performed according to manufacturer's instructions. Finally, Western (immuno-) blot analysis was carried out using primary antibodies against ZIP7 (Thermofisher, PA5-21072) ZnT7 (Santa Cruz, SC-160946). To confirm proper isolation of endoplasmic reticulum, SERCA-2 (Santa Cruz, SC-8094) was used as ER marker and 58K Golgi Protein (Abcam, ab-27043) was used as Golgi marker

ZIP7 knock-down in H9c2 cells with lentiviral stable infection

The H9c2 cells were stably transfected with 4 unique 29mer shRNA constructs in lentiviral RFP vector (Origene, SR02938179A, B, C and D) and Non-effective 29-mer scrambled shRNA cassette in pRFP-CB-shLenti Vector as a control (Origene, TR30033). Following 24 hours before the transfection, the HEK293T cells were seeded into separate dishes. Every

shRNA construct with packaging and enveloping plasmids (psPAX; Addgene 12260 and pMD2G; Addgene 12259) were mixed into a solution contained $CaCl_2$ (375 mM) and then incubated for 30 minutes at room temperature. Every DNA mixture was added into HBS buffer (containing as mM; 12 Dextrose, 50 HEPES, 10 KCl, 280 NaCl, 1.5 $Na_2HPO_4.H_2O$) as a drop wise manner while vortex and every mixture added into separate 15 cm dishes and incubated for 12 hours. Viral supernatants were harvested following 24 hours and 48 hours. The H9c2 cells were infected with each lentivirus produced from every shRNA construct including scrambled sequences at 3 PFU per cell. After infection, cells are incubated with medium contains blasticidin (10 µg/mL) for antibiotic selection. Then, the cells were seeded and into 6 well plates and harvested for determining the knocked-down efficiency by measuring the mRNA expression levels of ZIP7 (Supplementary Table I). For our experiments, we used the mixture of 4 ZIP7 gene specific shRNA constructs.

RNA Isolation and QRT-PCR Analysis

Total RNAs were prepared from isolated cardiomyocytes and H9c2 cells using an RNA Isolation Kit (Macherey–Nagel, 740955.10). Purified total RNA was reverse transcribed using ProtoScript First-Strand cDNA Synthesis Kit (New England Biolobs, E6300S). The resulting first strand cDNAs were quantified with GoTaq® qPCR Master Mix (Promega, A6001). As a housekeeping gene, β-actin (*Actb*) was used and expression results for all transcription factors were normalized with respect to β-actin mRNA levels. The amplified fragment size of the PCR products of each primer and the specificity of the primers were controlled with NCBI and ENSEMBL databases which are publicly available. The primer sequences for β-actin, ZIP7 and ZnT7 were listed in a Table given in Supplemental Materials. The fold changes in the expression of the genes were analyzed based on the comparative ($2^{-\Delta\Delta Ct}$) method.

Western (immuno-) blot Analysis

Frozen isolated cardiomyocytes and isolated sarco(endo)plasmic reticulum S(E)R fractions were pulverized at liquid nitrogen temperature and then homogenized. Cell lysates and tissues homogenates were extracted with NP-40 lysis buffer (250 mM NaCl, 1% NP-40, and 50 mM Tris-HCl; pH 8.0 and 1X PIC). The protein concentrations of supernatants after centrifugation (12,000×g, 5 minutes, at 4°C) were measured with the BCA assay kit (Pierce). Equal protein amounts were separated on 12% SDS-PAGE Tris-glycine or 4-12% Bis-Tris gels (Life Technologies). Proteins were transferred to PVDF membranes and blocked with 4% skimmed milk solution in PBS-Tween. Membranes were probed overnight with primary antibodies diluted in 4% skimmed milk solution in PBS-Tween. The membranes were probed with antibodies against GRP78 (Santa Cruz, sc-13968; 1:200), Calregulin (Santa Cruz, sc-11398; 1:200), ZIP7 (Santa Cruz, sc-83858; 1:200), ZnT7 (Santa Cruz,sc-160946; 1:200), SERCA-2 (Santa Cruz, sc-8094, 1:200), 58K Golgi Protein (Abcam, ab-27043; 1μg/ml), GAPDH (Santa Cruz,sc-365062; 1:1000) and β-actin (Santa Cruz, sc-47778; 1:500) in BSA/PBS/Tween-20 solution.

Specific bands were visualized with HRP-conjugated compatible secondary antibodies (anti-mouse: 1:2000, anti-goat: 1:7500, anti-rabbit: 1:7500) and detected by ImmunoCruz Western Blotting Luminol Reagent (Santa Cruz, sc-2048). The density of bands was analyzed using ImageJ software.

Co-immunoprecipitation Analysis

Cells were treated as indicated, lysed in co-immunoprecipitation (co-IP) buffer (50 mM Tris, pH 7.4, 100 mM NaCl, 1% Triton-X-100, 10% glycerol, 1 mM EDTA) containing protease inhibitors (1 mM PMSF, 1 μg/mL each of leupeptin, aprotinin and pepstatin) and phosphatase inhibitors (10 mM sodium fluoride, 1 mM sodium orthovanadate) for 30 minutes at 4°C with gentle shaking. The 600 μg protein lysates from aliquots (1 mL of lysis buffer) were pre-cleared via incubation with 30 μL of protein A/G Sepharose (Sigma, USA) for 1 hour at 4°C.

The pre-cleared samples were incubated with the specific primary antibody (anti-CK2α, 10 µg/mL; Santa Cruz, SC-6480) in lysis buffer for 2 hours at 4°C and then 30 µL of protein A/G beads were added. Following these procedures, the samples were incubated for overnight at 4°C and then the beads were washed five times with lysis buffer at 4°C and then boiled and separated by 10% SDS-PAGE. Finally, they were transferred onto a PVDF membrane followed by Western blotting analysis.

Data Analysis and Statistics

Data are presented as mean ± SEM unless otherwise stated. Differences were determined by using Student's t-test with Bonferroni correction for multiple comparisons as required, using GraphPad Prism 6.0. P-values < 0.05 were considered as statistically significant.

Results

Regulation of ZIP7 and ZnT7 Expression by High Glucose in Rat Cardiomyocytes

We aimed first to confirm the presence of both ZIP7 and ZnT7 in isolated cardiomyocytes by measuring their protein and mRNA levels under both physiological and chronic hyperglycemic (such as STZ-induced diabetic rats, DM group) conditions. The protein (right part) and mRNA (left part) levels of ZIP7 (at 50 kDa) and ZnT7 (at 42 kDa) measured in isolated rat ventricular cardiomyocytes are given in Fig. 1A and B. Both mRNA and protein (immunoreactivity) levels of ZIP7 were significantly increased in cardiomyocytes from diabetic rats whereas those of ZnT7 were found to be significantly decreased.

In order to test, a direct high glucose exposure to cardiomyocytes can induce the above changes, we incubated the isolated left ventricular cardiomyocytes with high glucose (33 mM) for 3 hours and then examined the protein and mRNA levels of both ZIP7 and ZnT7 comparison to those of mannitol (+23 mM) incubated cardiomyocytes. Their mRNA levels are changing as parallel to those of chronic hyperglycemic conditions (Supplementary Fig. 1)

while their protein levels are changed about 10% which is not statistically significant (data not shown). These differences may be due to not enough period high glucose incubation of the cells to induce changes in the protein levels. Of note, we did avoid to usage of longer incubation period for freshly isolated cells with high glucose.

In another set of experiments for further validation, we used high glucose (25 mM) incubated (24 hours) H9c2 cells and measured the protein and mRNA levels of ZIP7 and ZnT7. As can be seen from Fig. 1C and D, the protein and mRNA levels (Fig. 1C) of ZIP7 increased significantly in high glucose incubated H9c2 cells, while the ZnT7 mRNA level (Fig. 1D) is markedly (~75%) decreased with relatively small decrease (~25%) in its protein level.

High Glucose Induces Phosphorylation of ZIP7 in Cardiomyocytes

Since it has been previously shown a marked high phosphorylation level of ZIP7 by using a specific antibody developed by one of us (KT) in breast cancer cells (21), in this group of examinations, we aimed to examine a possible dependency of ZIP7 phosphorylation to hyperglycemia in both diabetic rat cardiomyocytes and high glucose incubated H9c2 cells (25 mM for 24 or 48 hours) comparison to non-incubated cells by Western blot analysis. As shown in Fig. 1 E and F, phospho-ZIP7 level measured at about 50 kDa in chronic hyperglycemic cells was about 7-fold higher comparison to the controls (A). Furthermore, the phospho-ZIP7 level in high glucose incubated H9c2 cells was high comparison to non-incubated cells, as a time-dependent manner, such as about 22% high in 24- our incubation and % in 48- our incubation (F; left and right, respectively).

Both ZIP7 and ZnT7 Localize to the Sarco(endo)plasmic Reticulum in H9c2 Cells

The expression levels of ZIP7 and ZnT7 have previously been reported in mammalian heart tissue(25; 26) and both have been proposed to localize to the ER membrane(20; 24; 28) and/or perinuclear vesicles associated with the Golgi apparatus(25; 27) in different types of cells.

Furthermore, it has been shown recently that endogenously expressed ZIP6 and ZIP7 are co-localized predominantly to the ER and regulate cytosolic Zn^{2+} homeostasis in dispersed pancreatic islet cells (22).

Therefore, we postulated first the similar endogenous subcellular localization for ZIP7 and ZnT7 as S(E)R in the H9c2 cardiac cells. To examine this postulate, the H9c2 cells were first transfacted with ER-resident Discosoma red fluorescent protein (DsRed-ER), then the cells were fixed and incubated with polyclonal antibodies to either ZIP7 or ZnT7 protein. DAPI was used to stain DNA in the nucleus. To visualize either ZIP7 or ZnT7 localization to the S(E)R, the ZIP7-specific and the ZnT7-specific antibodies and secondary antibodies were used. Individual and merged confocal microscopic images are shown in the four panels (Fig. 2A and B, respectively). The merge visual inspections can be attributed to the presence of the majority of ZIP7 and ZnT7 to the S(E)R. For colocalization values (the Pearson coefficient) calculated for ZIP7 and S(E)R and ZnT7 and S(E)R by using Huygens programme, are found as 0.67± 0.07 and 0.72±0.13, respectively.

To examine whether ZIP7 and ZnT7 localizes to Golgi apparatus, the H9c2 cells were co-incubated with GM130 and ZIP7 or ZnT7 antibodies and appropriate secondary antibodies. DAPI was again used to stain DNA in the nucleus. Individual and merged confocal microscopic images are shown in the four panels (Fig. 2C and D). The merge visual inspections can be attributed to the presence of minority of either ZIP7 or ZnT7 to the Golgi. For colocalization values (the Pearson coefficient) calculated for ZIP7 and Golgi and ZnT7 and Golgi by using Huygens programme, are found as 0.29±0.02 and 0.51±0.06, respectively.

DsRED-ER (red) plasmid transfected or non-transfected cells were incubated with only secondary antibodies and used to test the subcellular localisation for ZIP7 and ZnT7 without labeling to show nonspecific bounds. The nuclear DNA was stained with DAPI and all visual

images are presented for both S(E)R and Golgi testings in the four panels (Supplementary Fig. 2).

Demonstration of ZIP7 and ZnT7 Localizations Using Western (immuno-) Blot Analysis in Isolated S(E)R in H9c2 Cells

As a more direct assay, the localization of ZIP7 and ZnT7 on the S(E)R was further investigated by Western (immuno-) blot analysis of isolated S(E)R fractions (ranging from 1 to 14 in Figure 4B) obtained from rat heart homogenates. Immuno-blotting detected both ZIP7 and ZnT7 in all four fractions of S(E)R (Fig. 2E). The intensities of the immuno-cytochemical signal gradually increased moving from rough to smooth on the S(E)R for both transporters in these heart preparations. For validation of their presence in the S(E)R fractions, we also assessed SERCA2a levels in the same preparations, since this Ca^{2+}ATPase is located to the S(E)R membrane in mammalian cardiomyocytes (Figure 4B). As a negative control, we used a Golgi marker (Golgi-58K) in isolated S(E)R fractions. As can be seen from the same figure, we did not observe any protein band in this examination.

The above results confirm observations from the immunofluorescence examinations of localizations of ZIP7 and ZnT7 couple in the S(E)R of the rat heart.

FRET-based Measurement of Cytosolic and S(E)R Free Zn^{2+} Levels in Control and High Glucose-treated H9c2 Cells

Based on measurements of Zn^{2+} release during the cardiac cycle we have previously proposed a role for intracellular free Zn^{2+} in cardiomyocytesand implicated the S(E)R as an intracellular Zn^{2+} pool(4). In a later study, we demonstrated that the eCALWY family of genetically-encoded FRET Zn^{2+} probes (Cyt-eCALWY4 and ER-eCALWY6 for cytosol and S(E)R, respectively)(13; 39) permitted the measurements of free Zn^{2+} level in the S(E)R (5.6 ± 1.1 nM) and cytosol (0.61 ± 0.07 nM) in isolated rat ventricular cardiomyocytes, separately(13).

Here, using the same Zn^{2+} probes, we measured the free Zn^{2+} levels in the cytosol and S(E)R

in H9c2 cells after culture at normal (5.5 mM) or high (25 mM) glucose for 24 hours.

Representative free Zn^{2+} measurement protocols using the FRET probes in H9c2 cells and the

Zn^{2+}–chelator TPEN (50 µM) followed by the ionophore pyrithione (Pyr; 5 µM) plus $ZnCl_2$

(100 µM) are given in Fig. 3 (A for cytosol and B for S(E)R). Representative images, and the

protocols for calibration, are given on the left and middle parts of the figures. By using

quantification from fluorescence intensity-free Zn^{2+} concentration approach(13), we observed

that exposure of Cyt-eCALWY4-infected H9c2 to high glucose (25 mM for 24 hours) induced

significant increases in cytosolic free Zn^{2+} levels compared to cells cultiured at low glucose

(5.5 mM; from 0.97 ± 0.14 nM to 1.74 ± 0.15 nM, n=27 and 31 cells; p<0.05, 8 independent

experiments; right panels in Figure 1A and Figure 1B). However, we detected significantly

lower free Zn^{2+} concentrations in high glucose-treated and ER-eCALWY6 infected H9c2 cells

compared to the controls (from 4.88 ± 1.00 nM to 2.52 ± 0.36 nM, n=22 and 26 cells p<0.05,

8 independent experiments).

Re-distribution of Cellular Free Zn^{2+} in Cardiomyocytes under Hyperglycemia Depends on the state of ZIP7

The demonstration of ZIP7 and ZnT7 localization to the S(E)R in H9c2 cells provided further

evidence of a role for S(E)R as an intracellular Zn^{2+} pool in cardiomyocytes(4). Furthermore,

taken into consideration the relatively high mRNA and protein levels of ZIP7 together with its

significantly higher phosphorylation level under hyperglycemic conditions, we wanted to

assess its direct role in the redistribution of cellular free Zn^{2+} in hyperglycemic cells. We

therefore silenced ZIP7 in H9c2 cells. The mRNA expression levels of ZIP7 and ZnT7 in

these cells comparison to those of sc-shRNA cells are given in Fig. 4A and B (left,

respectively). ZIP7 mRNA level in these cells was reduced by >60% in comparison to control

cells while levels of ZnT7 mRNA were not changed. As expected, ZIP7 immunoreactivity

was reduced by >90 % in silenced cells while there was no change in ZnT7 protein levels (Fig. 4A and B, right, respectively).

To further test the role of ZIP7 in controlling the subcellular distribution of Zn^{2+}, we measured both cytosolic and S(E)R free Zn^{2+} levels in non-targeted shRNA-infected H9c2 cells using the genetically-encoded FRET-based Zn^{2+} probes Cyt-eCALWY4 or ER-eCALWY6, as described previously in sub-part 2 of the Results section. We analyzed cells maintained under physiological or hyperglycemic (25 mM glucose for 24 hours) conditions. As shown in Fig. 4C (left), cytosolic free Zn^{2+} was increased over 3-fold in hyperglycemic cells in comparison to the controls (from 0.92 ± 0.14 nM to 3.28 ± 0.65 nM; n=36-45, from 3 independent experiments). Furthermore, the cytosolic free Zn^{2+} level in ZIP7-silenced cells under hyperglycemia was not different from that of ZIP7 silenced cells under physiological conditions (Fig. 4C, right). However, the S(E)R free Zn^{2+} level in non-targeted shRNA infected cells expressing ER-eCALWY6 under hyperglycemia tended to decrease by about 36% (from 2.86 ± 0.48 nM to 1.82 ± 0.42; n=8-12, from 3 independent experiments; Fig. 4D, left). Furthermore, the free Zn^{2+} level in the S(E)R in ZIP7-silenced cells under hyperglycemia was not different from that of ZIP7 silenced cells under physiological conditions (Fig. 4D, right). These results are consistent with an important role for S(E)R-localized ZIP7 in the re-distribution of subcellular Zn^{2+} in cardiomyocytes under these pathological conditions.

Altered Protein Expression Level of ZIP7 and ZnT7 in Hyperglycemic Cardiomyocytes Cause ER-stress due to the Loss of S(E)R Free Zn^{2+}

Previously, we showed the presence of marked ER-stress and increased and increased intracellular free Zn^{2+} in freshly isolated left ventricular cardiomyocytes from diabetic rats(5; 34; 36). Importantly, these changes could be reversed by antioxidant treatment of the diabetic rats, significantly (5; 34; 36).

Of note, it has been demonstrated that Zn^{2+} deficiency in the ER disrupts organelle function and induces ER-stress in eukaryotes (17). We therefore hypothesized that similar changes in cardiomyocytes might also lead to ER-stress under hyperglycemic conditions. To test this prediction, we first measured the levels of two molecular chaperones involved in ER-stress, namely GRP78 and Calregulin (CALR) in high glucose (25 mM *vs.* 5.5 mM for 24 hours) incubated H9c2 cells in comparison to those of non-incubated controls. As shown in Fig. 5A (left and right), the protein levels of GRP78 and CALR were increased significantly in hyperglycemia-exposed cells, which are similar to those of previously observed data in diabetic rat heart (40).

In a further set of experiments we examined GRP78 induction in response to a direct ER-stress activator tunicamycin (TUN; 10 μM; 18 hours incubation). As shown in Fig. 5B, the GRP78 expression level was increased in TUN-incubated H9c2 cells. This finding can also support our previous data related with ER-stress chaperones GRP78 and CALR.

To demonstrate a hypothesis related with hyperglycemia-associated changes in protein expression levels of ZIP7 and ZnT7 can underlie the induction of ER-stress in cardiomyocytes, we used directly ER-stress induced cardiomyocytes with TUN-incubation and then measured the protein levels of these Zn^{2+}-transporters ZIP7 and ZnT7. As can be seen from Fig. 5C and D, the protein expression levels of both ZIP7 and ZnT7 measured in TUN-incubated cells were not different from those of controls, significantly. These last findings are also giving more support to our hypothesis of hyperglycemia associated changes in the protein expression levels of ZIP7 and ZnT7.

Phosphorylation of ZIP7 is a Direct Consequence of Hyperglycemia But not ER-Stress

Since we observed a markedly high phosphorylation level of ZIP7 in both chronic diabetic rat cardiaomyocytes (Fig. 1E) and high glucose incubated H9c2 cells as a time-dependent manner (Fig. 1F and G), we tested whether these changes may be a direct consequence of ER-stress.

17

We treated the H9c2 cells with 10 μM TUN to directly induce ER-stress and then measured phospho-ZIP7 levels. As can be seen in Fig. 5E, there were no significant differences between treated and untreated cells, implying no direct ER-stress effect on ZIP7 phosphorylation.

Activation of CK2 in Diabetic Cardiomyocytes is Associated with Hyperglycemia-Induced Increased Cytosolic Free Zn^{2+} levels

Since the protein kinase CK2 activation has recently been shown to prompt cytosolic Zn^{2+} signaling in a time-dependent manner[21], we examined the expression of CK2, firstly in isolated cardiomyocytes from left ventricle of diabetic rat heart. We also repeated the same measurements in Zn^{2+}/Pyr (1 μM; 20 minutes)-incubated the rat cardiomyocytes comparison to those of controls. As shown in Fig. 6A, CK2 immunoreactivity in both samples was significantly high comparison to the controls. Furthermore, we repeated the above measurements in cells maintained at either high glucose- (25 mM for 24 hours or 48 hours) or Zn^{2+}/Pyr- (1 μM for 20 minutes or 24 hours) incubated H9c2 cells. As can be seen from Fig. 6B, high glucose incubation of H9c2 cells for 24 hours induced significant CK2 activation (over 2-fold), in a time-dependent manner, because when the cells incubated with the same concentration of glucose for 48 hours, the activation was about 3.4-fold, which is significantly higher than that of 24 hours (data not given). Furthermore, when the H9c2 cells were incubated with 1 μM Zn^{2+}/Pyr for 20 minutes, the CK2 activation level was measured as over 8-fold high comparison to the control, however this activation was about 28% in 24 hours incubated H9c2 cells comparison to the control (data not given). These data demonstrate that CK2 expression is increased by hyperglycemia or elevated cytosolic free Zn^{2+}, and may contribute in a feed-forward cycle to further Zn^{2+} release into the cytoplasm. Most importantly, it should be emphasized that elevated cytosolic free Zn^{2+} effect on CK2 activation is time dependent and mostly developed in minutes rather than the hours.

CK2 Contributes to Activation of ZIP7 by Inducing ZIP7-phosphorylation in Hyperglycemia-exposed Cardiomyocytes

As recently reported(21) a CK2 activation-dependent ZIP7 phosphorylation and Zn^{2+} influx into the cytoplasm occurs from the ER in TamR cells. We therefore performed co-immunoprecipitation experiment in H9c2 cells by using a ZIP7-antibody and probed the precipitates for CK2 given their co-immunoprecipitation (Fig. 6C). These data, as shown previously as well, may reveal an association between CK2 activation and increased cytosolic free Zn^{2+}-dependent phosphorylation and activation of ZIP7 in response to hyperglycemia.

In order to test whether ZIP7 can be phosphorylated with other endogenous kinases, such as protein kinase A (PKA), protein kinase C (PKC) and calcium-calmodulin kinase II (CaMKII), which play important roles for the phosphorylation of several proteins in different endogenous signaling pathways and themselves also are phosphorylated with hyperglycemia as well as with increased intracellular free Zn^{2+} in cardiomyocytes (5; 36; 41), we performed co-immunoprecipitation experiment in H9c2 cells by using a ZIP7-antibody and probed the precipitates for every kinases to obtain their co-immunoprecipitation. Unfortunately, we could not obtain any co-immunoprecipitation for ZIP7 either with PKA, PKC, or CaMKII.

Discussion

The overall aim of this study was to examine the roles of the Zn^{2+} carriers ZIP7 and ZnT7 in cardiomyocytes under physiological conditions and as potential mediators of ER-stress in hyperglycemia and hyperglycemia-induced cardiac dysfunction. Our results suggest that ZIP7 and ZnT7 are likely to carry Zn^{2+} in opposite directions across the S(E)R membrane. Furthermore, we showed that increased ZIP7 levels were likely to drive changes in the S(E)R lumen and in the cytosol, with deleterious consequences for cell function in both cases. Although not assessed directly, lowered ZnT7 expression under conditions of hyperglycemia were likely to further exacerbate these changes and contribute to the deleterious consequences

of Zn^{2+} redistribution between compartments. Importantly, these two transporters were shown using both imaging and biochemical approaches to localize to the S(E)R membrane and may thus operate as a functional couple catalyzing Zn^{2+} release and uptake respectively from the S(E)R.

To the best of our knowledge, the current study is the first to be conducted to assess both the localization and the functional roles of ZIP7 and ZnT7 as working opposing direction in the mammalian heart and, most importantly, their contributions to diabetic cardiac dysfunction via ER-stress. Additionally, we demonstrate increased levels of CK2 expression under hyperglycemic conditions and provide evidence that this may lead to phosphorylation of the channel on residues previously implicated in the control of Zn^{2+} release (21). Thus, a combination of transcriptional and post-transcriptional mechanisms may contribute to ZIP7 activation in hyperglycemia and diabetes.

Our present findings also provide further evidence of a role for the S(E)R as an intracellular Zn^{2+} pool, contributing to Zn^{2+} regulation in cardiomyocytes, in a process controlled by ZIP7 and ZnT7. In this regard, it has shown how ER Zn^{2+} deficiency induces the unfolded protein response, UPR (17) and Zn^{2+} homeostasis is involved in UPR under stress conditions, via a putative Zn^{2+} transporter, localized to the ER(38). Moreover, and supporting the above findings, it has been demonstrated that high glucose is able to induce a stable increase in the cytosolic Zn^{2+} concentration in pancreatic β-cells and leads to profound alterations in the expression of genes important for Zn^{2+} homeostasis such as an increase in ZIP7 (2.4-fold) and ZIP8 (6.8-fold)(28). Therefore, our present observations are noteworthy when considering the important roles of ZIP7 and ZnT7 located to the S(E)R and responsible for ER-stress, in part, due to depressed S(E)R free Zn^{2+}.

It has been demonstrated that either a direct cytosolic free Zn^{2+} increase or under hyperglycemia in cardiomyocytes, similar to increased oxidative stress, could induce

markedly high phosphorylation in many endogenous kinases and oxidation of several proteins responsible for both electrical and mechanical activities of the heart (4; 5; 36; 42). This statement is consistent with recent studies on the role of ZIP7 in the control of Zn^{2+} release from S(E)R, resulting in the activation of multiple tyrosine kinases through Zn^{2+}-mediated inactivation of protein phosphatases in cancer cells (20; 21). Supporting these earlier findings, we show here that the protein kinase CK2 is activated in hyperglycemia-exposed cardiomyocytes, while it can be also activated directly with increased cytosolic free Zn^{2+}.

There are very little data to show the relation between intracellular free Zn^{2+}, Zn^{2+}-transporters and cardiovascular complications. In early studies, it has been demonstrated that Zn^{2+} transporter, ZIP7, is involved in the Zn^{2+} homeostasis of the Golgi apparatus (18). Although early studies have shown relatively weakly expressed ZIP7 and ZnT7 in mammalian heart tissue (25; 26), however, in here, we observed very strong protein expression levels of both ZIP7 and ZnT7 in diabetic rat heart tissue. Additionally, in previous studies, not in heart cells but in pancreatic beta cells, it is proposed that ZIP7 locates in the ER and to be involved in the release of Zn^{2+} from intracellular stores (20; 28).

Other studies have also demonstrated a correlation between increased reactive oxygen species (ROS), ER-stress and the CK2 activation in a human cell line (43; 44). Zn^{2+} distribution has previously proposed top be controlled via the CK2-mediated phosphorylation of ZIP7 (21). Furthermore, a protective role for ZnT7 against oxidative stress has also been proposed in mouse osteoblasts (45). Moreover, a high susceptibility to diet-induced glucose intolerance and insulin resistance has been demonstrated in ZnT7-null mice (27). The present studies represent the first investigation into the role of CK2-mediated phosphorylation of ZIP7 activity and its role in zinc homeostasis in the cardiac myocyte.

As discussed previously, hyperglycemia induces cardiac dysfunction due to increased oxidative stress and ER-stress (35; 37; 46). Our new data reinforce the prediction of a role for

S(E)R as an important Zn^{2+} pool in these cardiomyocytes, with ZIP7 and ZnT7 both localized to this organelle and making an important contribution to Zn^{2+} homeostasis. Nonetheless, we recognize that other Zn^{2+}-transporters (or Zn^{2+} binding proteins) may also contribute to the development of ER-stress in cardiomyocytes under pathological conditions. In this regard, mutations in the human *ZIP13* gene cause the spondylocheiro dysplastic form of Ehlers–Danlos syndrome, a heritable connective tissue disorder the result of vesicular Zn^{2+} trapping and ER Zn^{2+} deficiency rather than overload has been shown recently(47). Recent studies also provided compelling evidence that mutations inactivating one copy of ZnT8/*SLC30A8* reduce Type 2 diabetes risk in humans, and suggest that ZnT8 inhibition may be a novel therapeutic strategy in Type 2 diabetes prevention (15).

The present data provide important information related to Zn^{2+} homeostasis via a ZIP7 and ZnT7 functioning as opposing Zn^{2+}-transporters and localized to S(E)R in cardiomyocytes. This appears to function to maintain proper S(E)R function. Perturbed expression of either or both transporters may lead to altered Zn^{2+} distribution across the S(E)R membrane, leading to persistent ER stress, and possibly to other sequelae including apoptosis. Fig. 7 presents our hypothesis due to a summary of these present findings. Additionally, other contributors, including increased oxidative stress under hyperglycemia (this possibility has been discussed previously in a review article (48) may increase cytosolic free Zn^{2+} as a result of Zn^{2+} mobilization from metalloproteins (49). The latter might further stimulate ZIP7 activity and in turn, may lead to accelerated Zn^{2+} influx into the cytosol from the S(E)R.

As conclusion, in this study, we provided novel insights into the regulation of Zn^{2+} homeostasis in the heart and its role in hyperglycemia and diabetes-associated heart dysfunction. These findings may provide new targets, such as regulation of cellular Zn^{2+}, mediation of Zn^{2+}-transporters in this regulation, and protein kinase CK2 as endogenous target kinase against diabetes-induced cardiac dysfunction.

Duality of Interest

No potential conflicts relevant to this article were reported.

Authors Contributions

B.T. designed the study, wrote the manuscript, researched data, and provided funding for the study. G.A.R. supported the experimental data in his lab and reviewed and edited the manuscript. E.T. performed the electrophysiological and imaging experiments and contributed all biochemical and molecular biology experiments and analyzed the all experimental data and confocal images. V.B. and A.D. performed all biochemical and molecular experiments. G.R.J.C. contributed to knock down experiments. K.T. provided the antibody for ZIP7 and contributed to the discussion. B.T. is the guarantor of this work and, as such, had full access

to all the data in the study and takes responsibility for the integrity of the data and the accuracy of the data analysis.

Prior Presentation

Parts of this study were presented in abstract form at the 2016 Biophysical Society 60th Annual Meeting, Los Angeles, CA, February 27 – March 04, 2016.

This article contains Supplementary Documents Online at

http://diabetes.diabetesjournals.org

References

1. Fein FS, Kornstein LB, Strobeck JE, Capasso JM, Sonnenblick EH: Altered myocardial mechanics in diabetic rats. Circ Res 1980;47:922-933
2. Choi KM, Zhong Y, Hoit BD, Grupp IL, Hahn H, Dilly KW, Guatimosim S, Lederer WJ, Matlib MA: Defective intracellular Ca(2+) signaling contributes to cardiomyopathy in Type 1 diabetic rats. Am J Physiol Heart Circ Physiol 2002;283:H1398-1408
3. Yaras N, Ugur M, Ozdemir S, Gurdal H, Purali N, Lacampagne A, Vassort G, Turan B: Effects of diabetes on ryanodine receptor Ca release channel (RyR2) and Ca2+ homeostasis in rat heart. Diabetes 2005;54:3082-3088
4. Tuncay E, Bilginoglu A, Sozmen NN, Zeydanli EN, Ugur M, Vassort G, Turan B: Intracellular free zinc during cardiac excitation-contraction cycle: calcium and redox dependencies. Cardiovasc Res 2011;89:634-642
5. Tuncay E, Okatan EN, Vassort G, Turan B: ss-blocker timolol prevents arrhythmogenic Ca(2)(+) release and normalizes Ca(2)(+) and Zn(2)(+) dyshomeostasis in hyperglycemic rat heart. PLoS One 2013;8:e71014
6. Turan B, Fliss H, Desilets M: Oxidants increase intracellular free Zn2+ concentration in rabbit ventricular myocytes. Am J Physiol 1997;272:H2095-2106
7. Tuncay E, Turan B: Intracellular Zn(2+) Increase in Cardiomyocytes Induces both Electrical and Mechanical Dysfunction in Heart via Endogenous Generation of Reactive Nitrogen Species. Biol Trace Elem Res 2016;169:294-302
8. Ayaz M, Turan B: Selenium prevents diabetes-induced alterations in [Zn2+]i and metallothionein level of rat heart via restoration of cell redox cycle. Am J Physiol Heart Circ Physiol 2006;290:H1071-1080
9. Atar D, Backx PH, Appel MM, Gao WD, Marban E: Excitation-transcription coupling mediated by zinc influx through voltage-dependent calcium channels. J Biol Chem 1995;270:2473-2477
10. Hirano T, Murakami M, Fukada T, Nishida K, Yamasaki S, Suzuki T: Roles of zinc and zinc signaling in immunity: zinc as an intracellular signaling molecule. Adv Immunol 2008;97:149-176
11. Wieringa FT, Dijkhuizen MA, Fiorentino M, Laillou A, Berger J: Determination of zinc status in humans: which indicator should we use? Nutrients 2015;7:3252-3263
12. Woodier J, Rainbow RD, Stewart AJ, Pitt SJ: Intracellular Zinc Modulates Cardiac Ryanodine Receptor-mediated Calcium Release. J Biol Chem 2015;290:17599-17610
13. Chabosseau P, Tuncay E, Meur G, Bellomo EA, Hessels A, Hughes S, Johnson PR, Bugliani M, Marchetti P, Turan B, Lyon AR, Merkx M, Rutter GA: Mitochondrial and ER-targeted eCALWY probes reveal high levels of free Zn2+. ACS Chem Biol 2014;9:2111-2120

14. Kambe T, Tsuji T, Hashimoto A, Itsumura N: The Physiological, Biochemical, and Molecular Roles of Zinc Transporters in Zinc Homeostasis and Metabolism. Physiol Rev 2015;95:749-784

15. Chabosseau P, Rutter GA: Zinc and diabetes. Arch Biochem Biophys 2016;

16. Kimura T, Kambe T: The Functions of Metallothionein and ZIP and ZnT Transporters: An Overview and Perspective. Int J Mol Sci 2016;17

17. Ellis CD, Wang F, MacDiarmid CW, Clark S, Lyons T, Eide DJ: Zinc and the Msc2 zinc transporter protein are required for endoplasmic reticulum function. J Cell Biol 2004;166:325-335

18. Huang L, Kirschke CP, Zhang Y, Yu YY: The ZIP7 gene (Slc39a7) encodes a zinc transporter involved in zinc homeostasis of the Golgi apparatus. J Biol Chem 2005;280:15456-15463

19. Hogstrand C, Kille P, Nicholson RI, Taylor KM: Zinc transporters and cancer: a potential role for ZIP7 as a hub for tyrosine kinase activation. Trends Mol Med 2009;15:101-111

20. Taylor KM, Vichova P, Jordan N, Hiscox S, Hendley R, Nicholson RI: ZIP7-mediated intracellular zinc transport contributes to aberrant growth factor signaling in antihormone-resistant breast cancer Cells. Endocrinology 2008;149:4912-4920

21. Taylor KM, Hiscox S, Nicholson RI, Hogstrand C, Kille P: Protein kinase CK2 triggers cytosolic zinc signaling pathways by phosphorylation of zinc channel ZIP7. Sci Signal 2012;5:ra11

22. Liu Y, Batchuluun B, Ho L, Zhu D, Prentice KJ, Bhattacharjee A, Zhang M, Pourasgari F, Hardy AB, Taylor KM, Gaisano H, Dai FF, Wheeler MB: Characterization of Zinc Influx Transporters (ZIPs) in Pancreatic beta Cells: ROLES IN REGULATING CYTOSOLIC ZINC HOMEOSTASIS AND INSULIN SECRETION. J Biol Chem 2015;290:18757-18769

23. Grubman A, Lidgerwood GE, Duncan C, Bica L, Tan JL, Parker SJ, Caragounis A, Meyerowitz J, Volitakis I, Moujalled D, Liddell JR, Hickey JL, Horne M, Longmuir S, Koistinaho J, Donnelly PS, Crouch PJ, Tammen I, White AR, Kanninen KM: Deregulation of subcellular biometal homeostasis through loss of the metal transporter, Zip7, in a childhood neurodegenerative disorder. Acta Neuropathol Commun 2014;2:25

24. Groth C, Sasamura T, Khanna MR, Whitley M, Fortini ME: Protein trafficking abnormalities in Drosophila tissues with impaired activity of the ZIP7 zinc transporter Catsup. Development 2013;140:3018-3027

25. Kirschke CP, Huang L: ZnT7, a novel mammalian zinc transporter, accumulates zinc in the Golgi apparatus. J Biol Chem 2003;278:4096-4102

26. Yang J, Zhang Y, Cui X, Yao W, Yu X, Cen P, Hodges SE, Fisher WE, Brunicardi FC, Chen C, Yao Q, Li M: Gene profile identifies zinc transporters differentially expressed in normal human organs and human pancreatic cancer. Curr Mol Med 2013;13:401-409

27. Huang L, Kirschke CP, Lay YA, Levy LB, Lamirande DE, Zhang PH: Znt7-null mice are more susceptible to diet-induced glucose intolerance and insulin resistance. J Biol Chem 2012;287:33883-33896

28. Bellomo EA, Meur G, Rutter GA: Glucose regulates free cytosolic Zn(2)(+) concentration, Slc39 (ZiP), and metallothionein gene expression in primary pancreatic islet beta-cells. J Biol Chem 2011;286:25778-25789

29. Rungby J: Zinc, zinc transporters and diabetes. Diabetologia 2010;53:1549-1551

30. Kambe T, Fukue K, Ishida R, Miyazaki S: Overview of Inherited Zinc Deficiency in Infants and Children. J Nutr Sci Vitaminol (Tokyo) 2015;61 Suppl:S44-46

31. Rutter GA, Chabosseau P, Bellomo EA, Maret W, Mitchell RK, Hodson DJ, Solomou A, Hu M: Intracellular zinc in insulin secretion and action: a determinant of diabetes risk? Proc Nutr Soc 2016;75:61-72

32. Li F, Luo J, Wu Z, Xiao T, Zeng O, Li L, Li Y, Yang J: Hydrogen sulfide exhibits cardioprotective effects by decreasing endoplasmic reticulum stress in a diabetic cardiomyopathy rat model. Mol Med Rep 2016;14:865-873

33. Yang L, Zhao D, Ren J, Yang J: Endoplasmic reticulum stress and protein quality control in diabetic cardiomyopathy. Biochim Biophys Acta 2015;1852:209-218

34. Cicek FA, Ozgur EO, Ozgur E, Ugur M: The interplay between plasma membrane and endoplasmic reticulum Ca(2+)ATPases in agonist-induced temporal Ca(2+) dynamics. J Bioenerg Biomembr 2014;46:503-510

35. Lakshmanan AP, Harima M, Suzuki K, Soetikno V, Nagata M, Nakamura T, Takahashi T, Sone H, Kawachi H, Watanabe K: The hyperglycemia stimulated myocardial endoplasmic reticulum (ER) stress contributes to diabetic cardiomyopathy in the transgenic non-obese type 2 diabetic rats: a differential role of unfolded protein response (UPR) signaling proteins. Int J Biochem Cell Biol 2013;45:438-447

36. Tuncay E, Okatan EN, Toy A, Turan B: Enhancement of cellular antioxidant-defence preserves diastolic dysfunction via regulation of both diastolic Zn2+ and Ca2+ and prevention of RyR2-leak in hyperglycemic cardiomyocytes. Oxid Med Cell Longev 2014;2014:290381

37. Harding HP, Ron D: Endoplasmic reticulum stress and the development of diabetes: a review. Diabetes 2002;51 Suppl 3:S455-461

38. Wang M, Xu Q, Yu J, Yuan M: The putative Arabidopsis zinc transporter ZTP29 is involved in the response to salt stress. Plant Mol Biol 2010;73:467-479

39. Vinkenborg JL, Nicolson TJ, Bellomo EA, Koay MS, Rutter GA, Merkx M: Genetically encoded FRET sensors to monitor intracellular Zn2+ homeostasis. Nat Methods 2009;6:737-740

40. Cicek FA, Toy A, Tuncay E, Can B, Turan B: Beta-blocker timolol alleviates hyperglycemia-induced cardiac damage via inhibition of endoplasmic reticulum stress. J Bioenerg Biomembr 2014;46:377-387

41. Yaras N, Tuncay E, Purali N, Sahinoglu B, Vassort G, Turan B: Sex-related effects on diabetes-induced alterations in calcium release in the rat heart. Am J Physiol Heart Circ Physiol 2007;293:H3584-3592

42. Xie H, Zhu PH: Biphasic modulation of ryanodine receptors by sulfhydryl oxidation in rat ventricular myocytes. Biophys J 2006;91:2882-2891

43. Intemann J, Saidu NE, Schwind L, Montenarh M: ER stress signaling in ARPE-19 cells after inhibition of protein kinase CK2 by CX-4945. Cell Signal 2014;26:1567-1575

44. Welker S, Gotz C, Servas C, Laschke MW, Menger MD, Montenarh M: Glucose regulates protein kinase CK2 in pancreatic beta-cells and its interaction with PDX-1. Int J Biochem Cell Biol 2013;45:2786-2795

45. Liang D, Xiang L, Yang M, Zhang X, Guo B, Chen Y, Yang L, Cao J: ZnT7 can protect MC3T3-E1 cells from oxidative stress-induced apoptosis via PI3K/Akt and MAPK/ERK signaling pathways. Cell Signal 2013;25:1126-1135

46. Bhandary B, Marahatta A, Kim HR, Chae HJ: An involvement of oxidative stress in endoplasmic reticulum stress and its associated diseases. Int J Mol Sci 2012;14:434-456

47. Jeong J, Walker JM, Wang F, Park JG, Palmer AE, Giunta C, Rohrbach M, Steinmann B, Eide DJ: Promotion of vesicular zinc efflux by ZIP13 and its implications for spondylocheiro dysplastic Ehlers-Danlos syndrome. Proc Natl Acad Sci U S A 2012;109:E3530-3538

48. Vassort G, Turan B: Protective role of antioxidants in diabetes-induced cardiac dysfunction. Cardiovasc Toxicol 2010;10:73-86

49. Fliss H, Menard M: Oxidant-induced mobilization of zinc from metallothionein. Arch Biochem Biophys 1992;293:195-199

Figure legends

Fig. 1. The mRNA expression and protein levels of ZIP7 and ZnT7 in cardiomyocytes from either diabetic rat heart or hyperglycemic H9c2 cells. The mRNA and protein levels of ZIP7 (A) and ZnT7 (B) in ventricular cardiomyocytes isolated from either diabetic (DM) or

control (CON) rats (see Methods). The mRNA expression and protein levels of ZIP7 (C) and

ZnT7 (D) from high glucose incubated (25 mM *vs* 5.5 mM for 24 hours) H9c2 cells.

Densitometric analysis showing (upper part of the bars) ZIP7 and ZnT7 are expressed at ~50

kDa and 42 kDa, respectively. The ZIP7 phosphorylation in cardiomyocytes under chronic

hyperglycemia (diabetic rat cardiomyocytes; DM group) comparison to the controls (CON)

(E), and H9c2 cells incubated with high glucose, HG (25 mM for 24 or 48 hours) (F; left and

right). The phosphorylation levels of ZIP7 are measured by using phospho-ZIP7 antibody

developed by KT Lab and given with comparison to their controls. Bars represent mean

(±SEM). Number of samples, *n*=5–6 for hearts/group/protocol and measurements with double

assays in each sample from each group for each type of measurement. Significance level

accepted at *p<0.05 *vs* CON.

Fig. 2. Visualization of ZIP7 and ZnT7 localization to the sarco(endo)plasmic reticulum

in H9c2 cells. Localizations of either ZIP7 (A) or ZnT7 (B) to either the S(E)R or Golgi

apparatus (C and D, respectively) were visualized by using confocal micrographs in H9c2

cells. To examine the subcellular localizations of ZIP7 or ZnT7 to S(E)R, H9c2 cells were

transfected with ER-resident Discosoma red fluorescent protein (DsRed- ER) to label ER or

incubated with GM130 antibody to label Golgi apparatus. All cells were fixed and

permeabilized (see Research Design and Methods). DsRed-ER transfected cells incubated

with specific either ZIP7 or ZnT7 primary antibodies and followed by secondary antibodies

(Alexa Fluor 488 Donkey anti-Rabbit IgG or Alexa Fluor 488 Donkey anti-Goat IgG,

respectively). To test their possible Golgi localizations (C and D), the non-transfected cells

were incubated with either ZIP7 or ZnT7 primary antibodies and GM130 primary antibody,

and then followed by secondary antibodies (Alexa Fluor 488 Donkey anti-Rabbit IgG and

Alexa Fluor 568 Goat anti-Mouse IgG or Alexa Fluor 488 Donkey anti-Goat IgG and Alexa

Fluor 568 Rabbit anti-Mouse IgG, respectively). The cells were mounted medium containing

DAPI (blue; to stain nuclei). Single optical sections (upper panels) and representative z-plane reconstructions (side and lower panels) are shown. The insets in right hand side panels show a magnified region. Bar, 10-μm. For colocalization values, the Pearson coefficients calculated for ZIP7 and S(E)R as well as ZnT7 and S(E)R by using the Huggens programme (see Materials and Methods), were 0.67 ± 0.07 and 0.72 ± 0.13, respectively. (E) Either ZIP7 or ZnT7 individual localization to the S(E)R was investigated with Western (immuno)-blot analysis in isolated S(E)R fractions (fractions from 1 to 14). Immunoblotting detected either ZIP7 or ZnT7 in all four fractions containing S(E)R membranes. For validation of S(E)R localization of ZIP7 and ZnT7, 58K Golgi Protein (Abcam, ab-27043) was used as Golgi marker.

Fig. 3. FRET-based measurements of subcellular free Zn^{2+} concentrations in hyperglycemic H9c2 cells using eCALWY probes. Representative traces (upper part) and ratiometric images (lower) are shown for H9c2 cells expressing cytosolic (A) or ER-targeted (B) sensors. Acquisitions were performed 24 hours after transfection or infection and during perfusion with Krebs-HEPES-bicarbonate (KHB) buffer. Steady state fluorescence intensity ratio (citrine/cerulean) was first measured before the maximum ratio was obtained under perfusion with KHB buffer containing 50 μM TPEN. Finally, the minimum ratio was obtained under perfusion with KHB buffer containing 5 μM Zn^{2+}-pyrithione (Zn^{2+}/Pyr) and 100 μM $ZnCl_2$ (Zn^{2+}-saturated condition). Cells were incubated with high glucose (HG; 25 mM for 24 hours) and the cytosolic and ER free Zn^{2+} levels are given comparison to the controls (CON). Bars represent mean (±SEM) and *n*>20 cells in every protocol. Significance level accepted at *p<0.05 *vs* CON.

Fig. 4. Confirmation of ZIP7 silencing and FRET-based measurements of cytosolic or S(E)R free Zn^{2+} concentrations in H9c2 cells cultured under hyper- or normo-glycemic conditions. The ZIP7 silencing was confirmed by measuring ZIP7 and ZnT7 mRNA (A) and
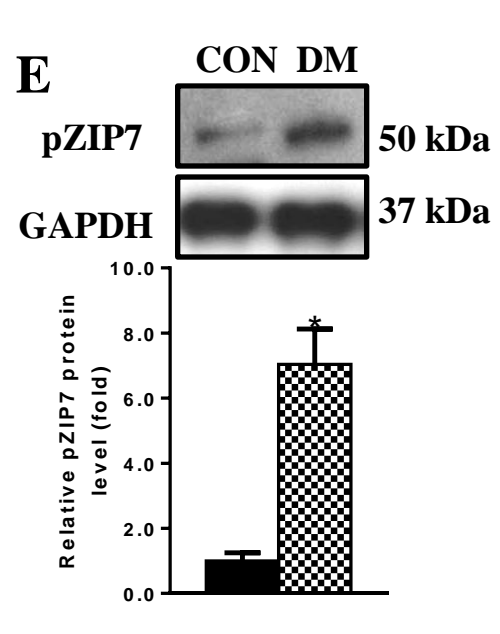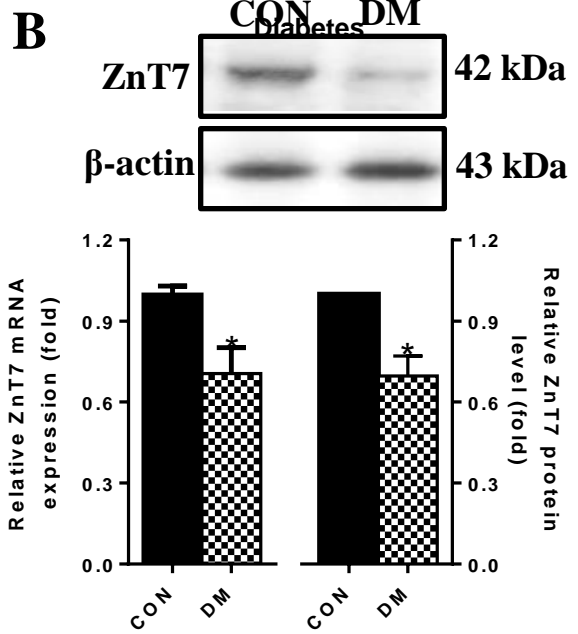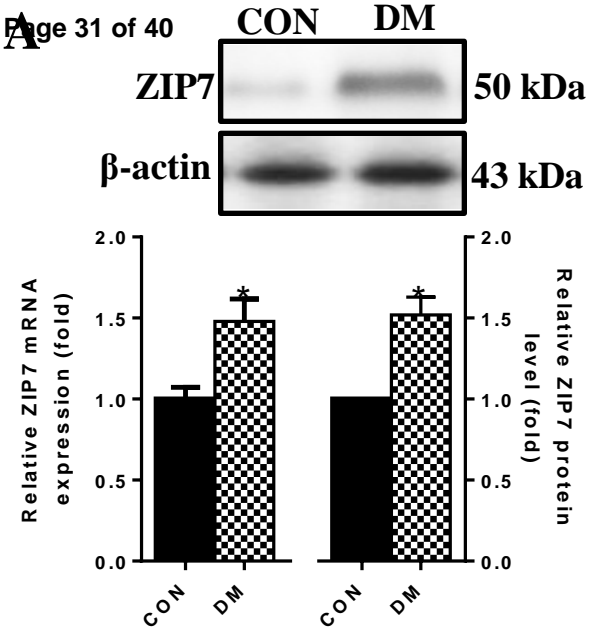
protein (B) levels with respect to scrambled shRNA-infected cells. ZIP7 silencing does not

affect ZnT7 mRNA (A; right) or protein (B; right) levels. The cytosolic (C) and S(E)R (D)

free Zn^{2+} levels measured in ZIP7 silenced H9c2 cells under hyperglycemic conditions using

expressed eCALWY sensors (FRET measurements were carried out as for Fig. 3) and

comparison to those in scrambled shRNA-treated cells. Bars represent mean (±SEM) and

n=8-36 cells for each protocol. Significance level accepted at *p<0.05 *vs* scramble-cells.

Fig. 5. The *in vitro* induction and confirmation of ER-stress in H9c2 cells. To test whether

hyperglycemia induces changes in the protein levels of ZIP7 and ZnT7 and then turns to

further underlie the induction of ER-stress in H9c2 cells, two molecular chaperones, GRP78

(A, left) and calregulin (CALR; A, right) are measured by Western (immuno-) blotting, in

H9c2 cells incubated with either high glucose (HG; 25 mM, 24 hours). (B) GRP78 measured

under directly ER-stress induction with tunicamycin (TUN). Protein levels of ZIP7 (C) and

ZnT7 (D) were measured after ER-stress induction with TUN. (E) Phospho-ZIP7 protein level

was measured in H9c2 cells incubated with TUN with respect to GAPDH as reference

protein. Bars represent mean (±SEM) and data were obtained after duplicate assays of each

sample from each group for each type of measurement. Significance level accepted at *p<0.05

vs CON.

Fig. 6. Activated CK2 in diabetic rat heart cells and high glucose- or Zn^{2+}-ionophore

incubated-H9c2 cells and demonstration of colocalization of CK2 and ZIP7. (A) The

protein level of protein kinase CK2 measured at 43 kDa in cardiomyocytes from normal

(CON) and diabetic (DM) rats, and isolated cardiomyocytes incubated with an ionophore

Zn^{2+}-pyrithione (Zn^{2+}/Pyr; 1 μM for 20 minutes). (B) H9c2 cells incubated either with high

glucose (HG; 25 mM for 24 hours) or Zn^{2+}/Pyr (1 μM for 20 minutes). (C) To determine

whether ZIP7 phosphorylation is associated with CK2 activation or *vice versa* in

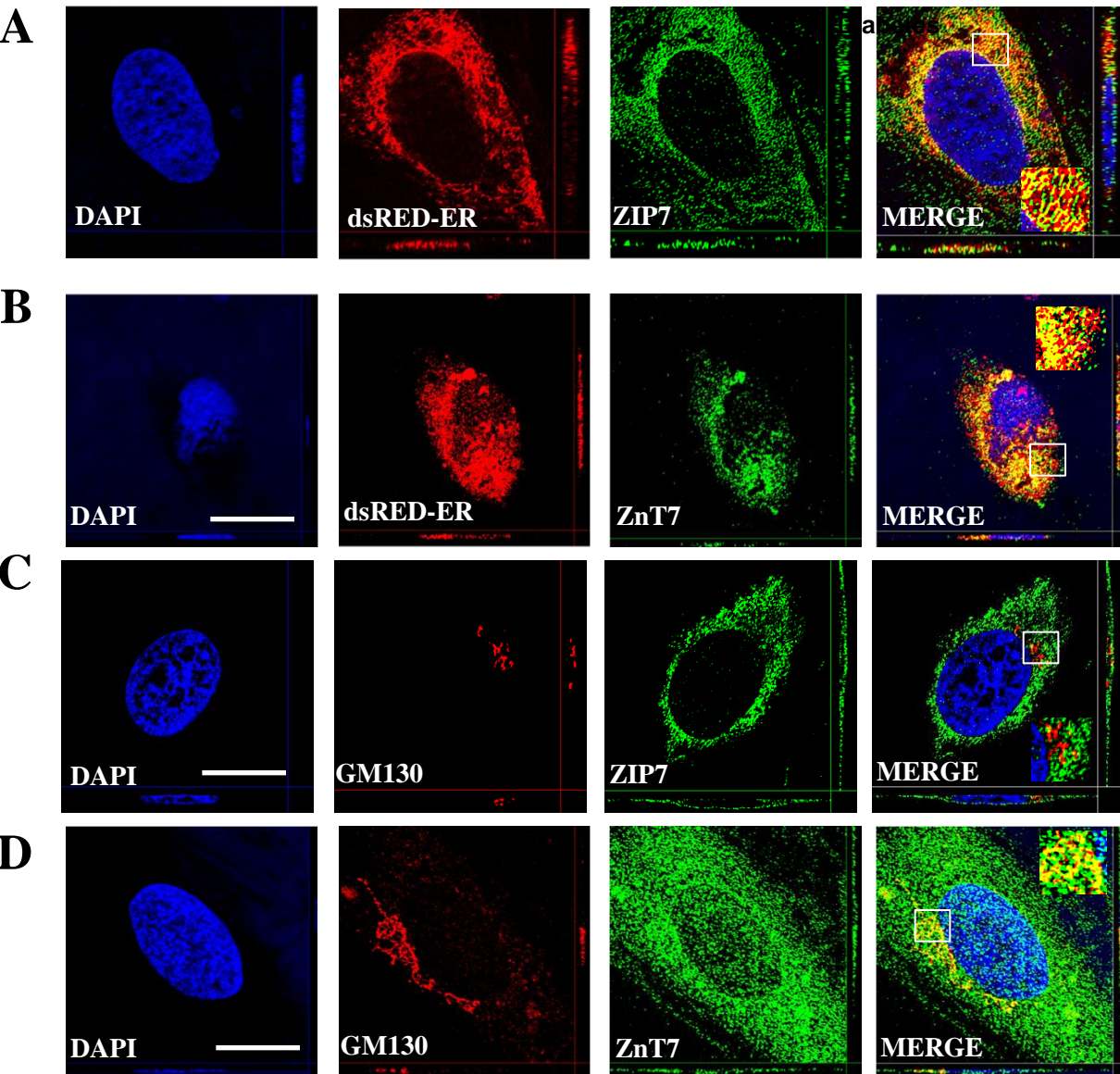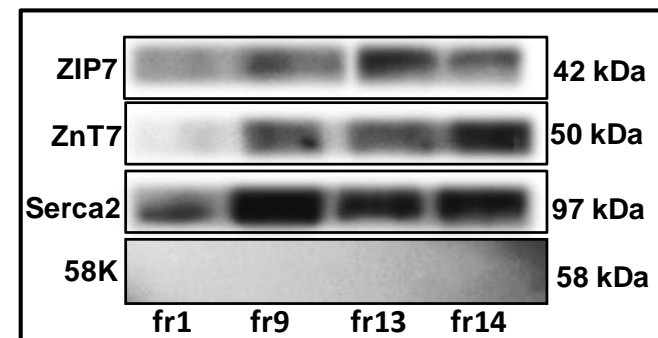hyperglycemia-exposed cells, co-immunoprecipitation experiments were performed using

anti-ZIP7 antibody and probed the precipitates for CK2 in H9c2 cells. The bars are given as mean (±SEM) and data obtained with double assays in each sample from each group for each type of measurement. Significance level accepted at *p<0.05 *vs* CON.

Fig. 7. Schematic illustration of the regulation of Zn^{2+} homeostasis in cardiomyocytes under physiological and hyperglycemic conditions. (A) Regulation of cellular distribution of free Zn^{2+} via a ZIP7 and ZnT7 system localized to the sarco(endo)plasmic reticulum [S(E)R] in resting cardiomyocytes. (B) Hyperglycemia can stimulate an increase of cytosolic free Zn^{2+} in cardiomyocytes as a result of the mobilization of Zn^{2+} from metalloproteins. This increase can induce either directly ER-stress via inducing overexpression of ER-stress chaperons or up-regulation of CK2, which, in turn, leads to activation of CK2 inducing Zn^{2+} influx into the cytosol from the S(E)R. Phosphorylation of ZIP7(21) and downregulation of ZnT7 may further contribute to these changes.
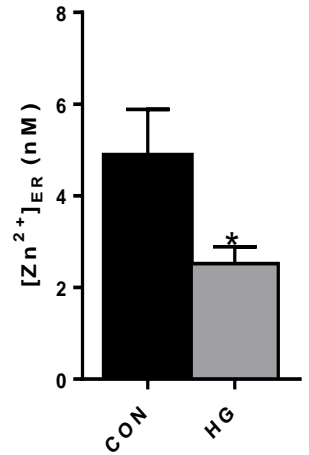
Fig.1

Fig. 2

Fig. 3

Fig. 4

A

CON HG   CON HG (Diabetes)   **B** CON +TUN

GRP78   78 kDa   CALR   55 kDa   GRP78   78 kDa

β-actin   43 kDa   β-actin   43 kDa   β-actin   43 kDa

C CON +TUN   **D** CON +TUN   **E** CON +TUN

ZIP7   55 kDa   ZnT7   42 kDa   pZIP7   50 kDa

β-actin   43 kDa   β-actin   43 kDa   GAPDH   37 kDa
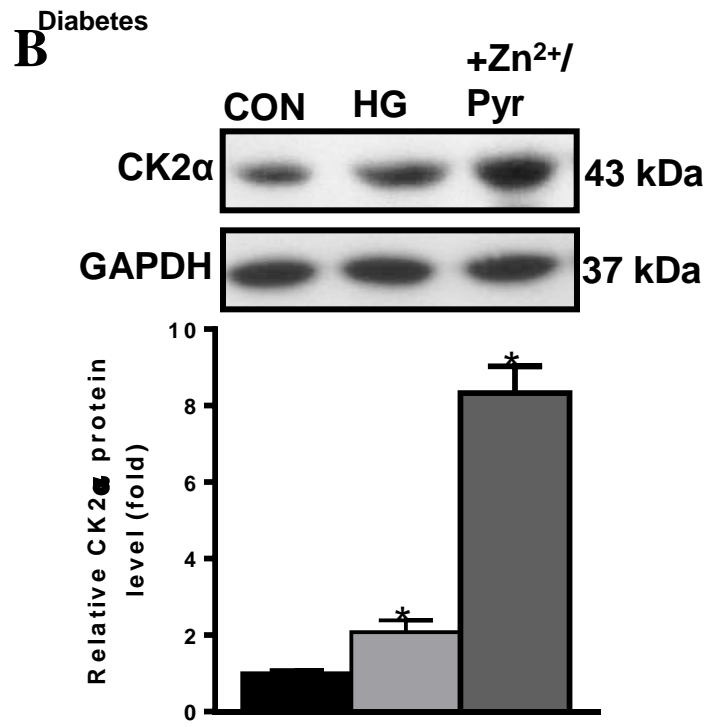
Fig. 5

A

B
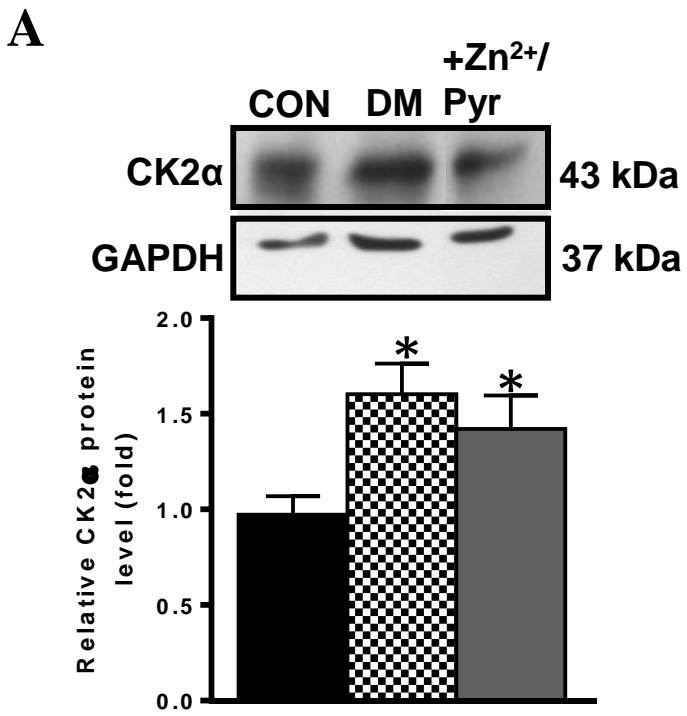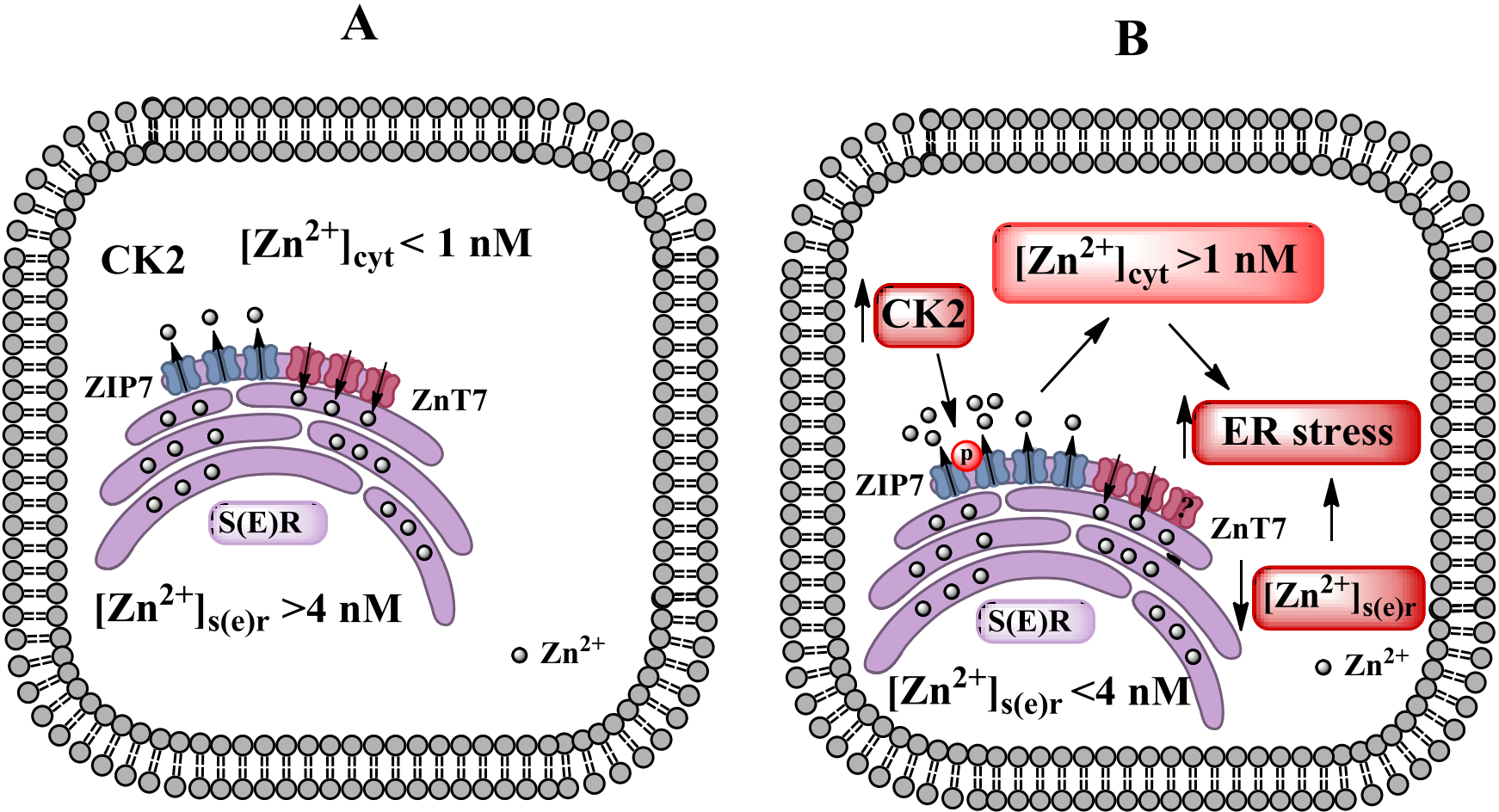
C
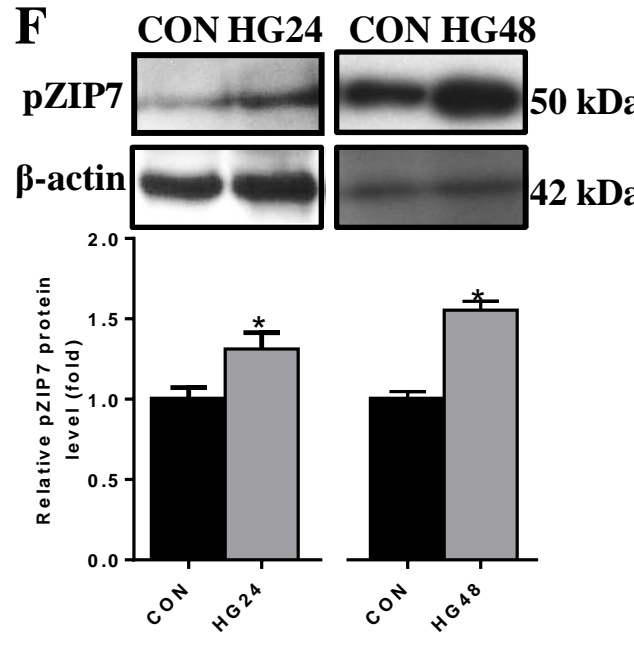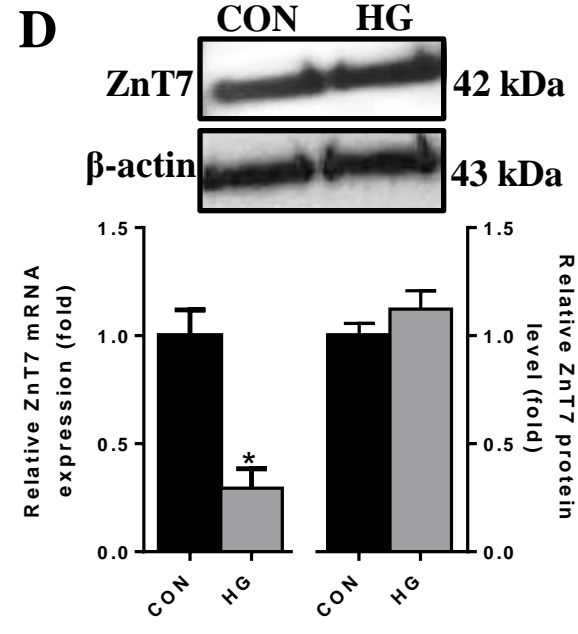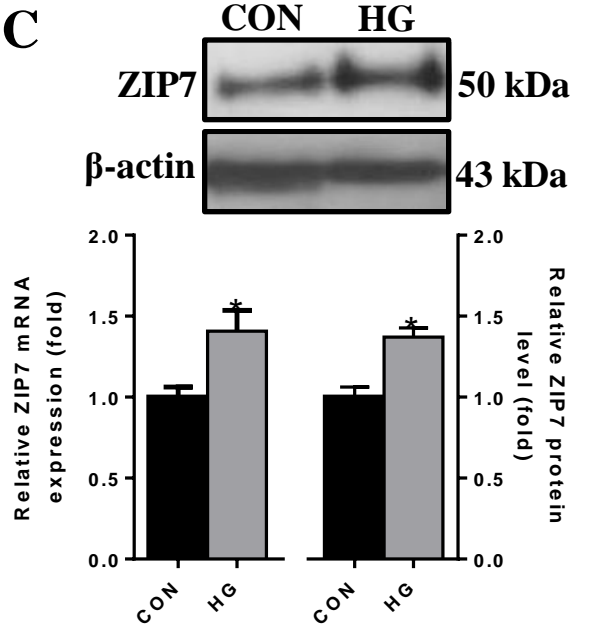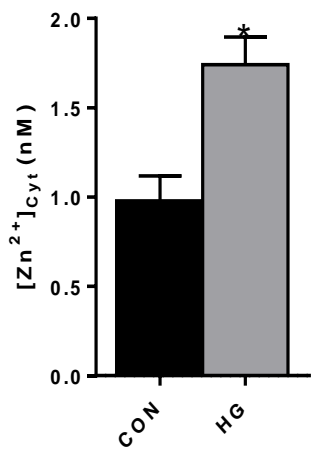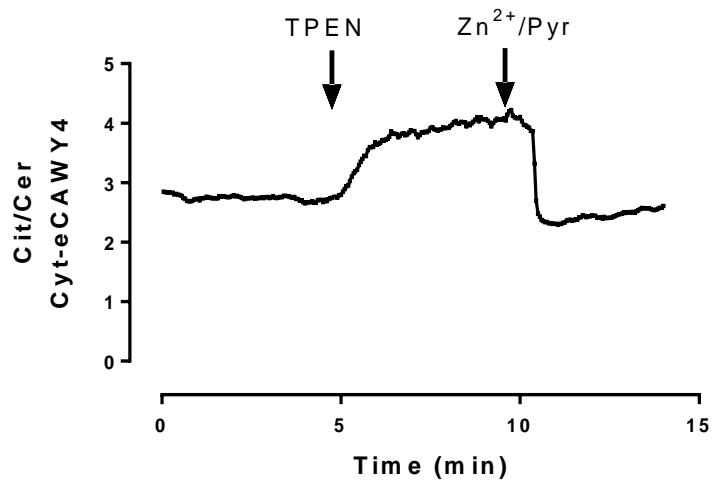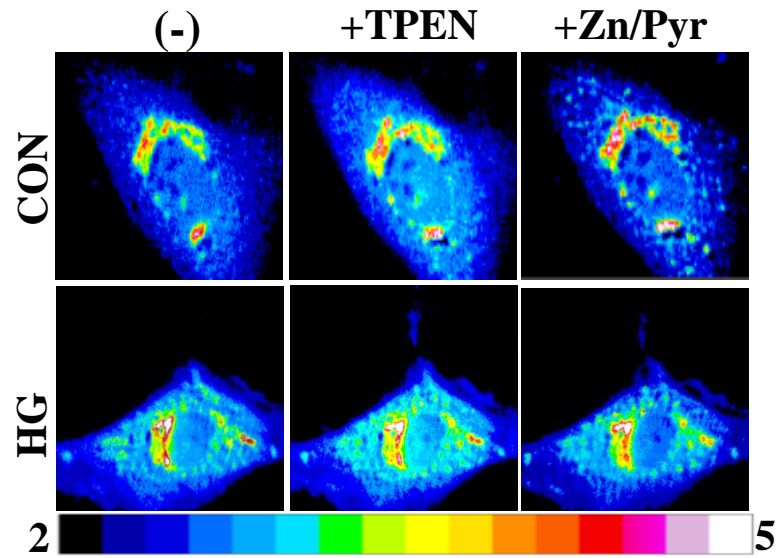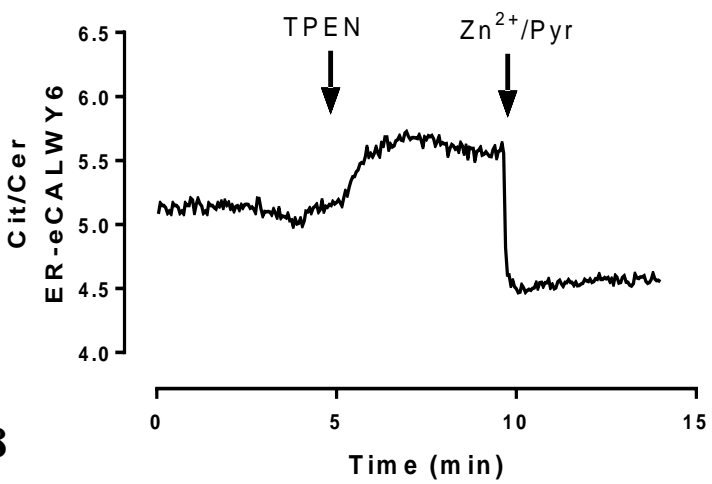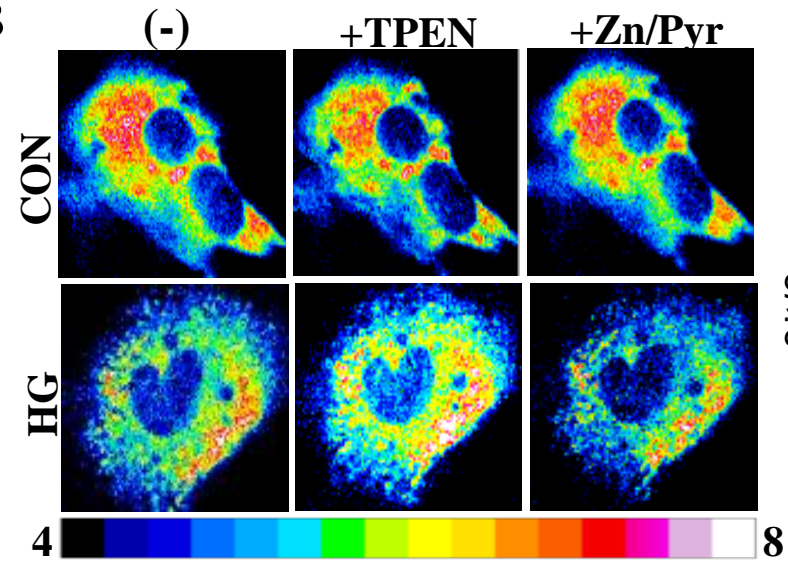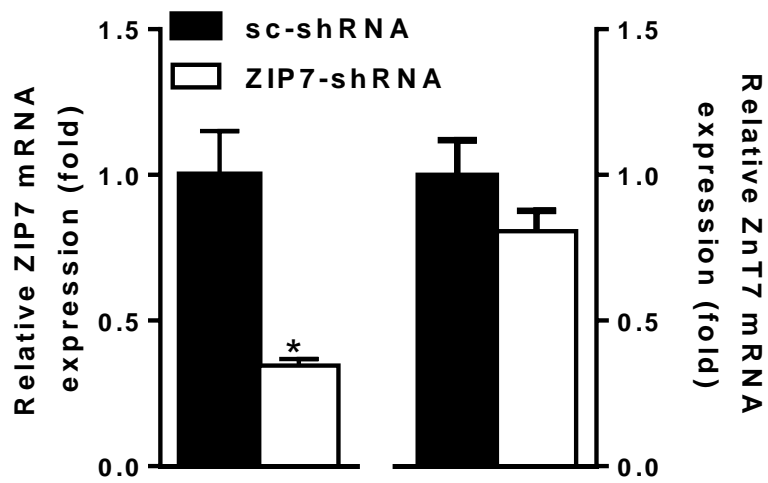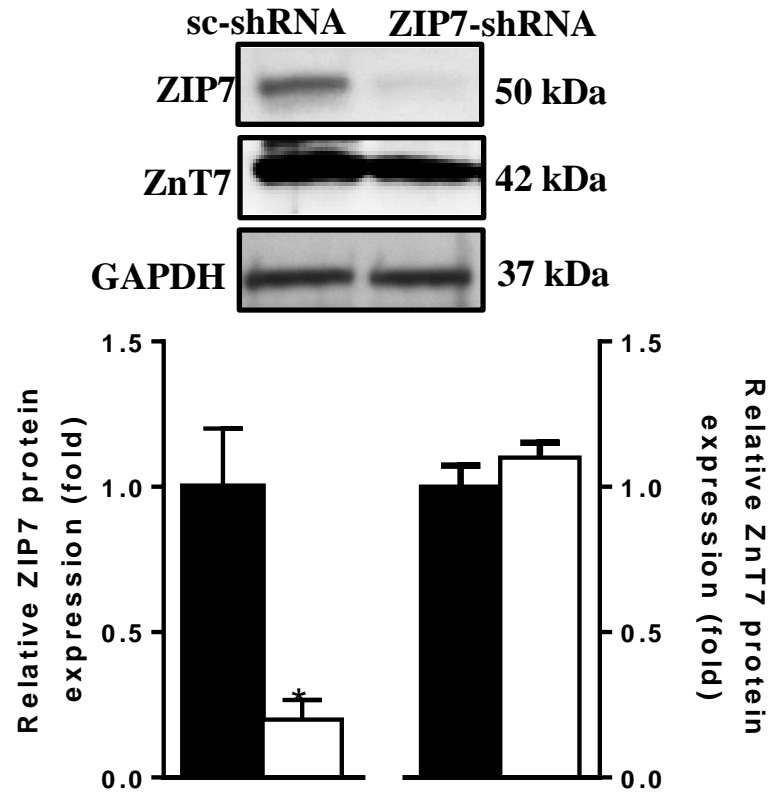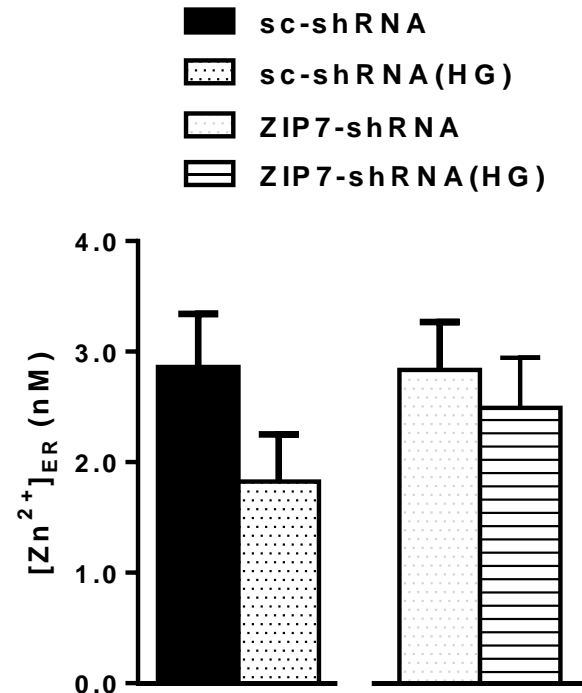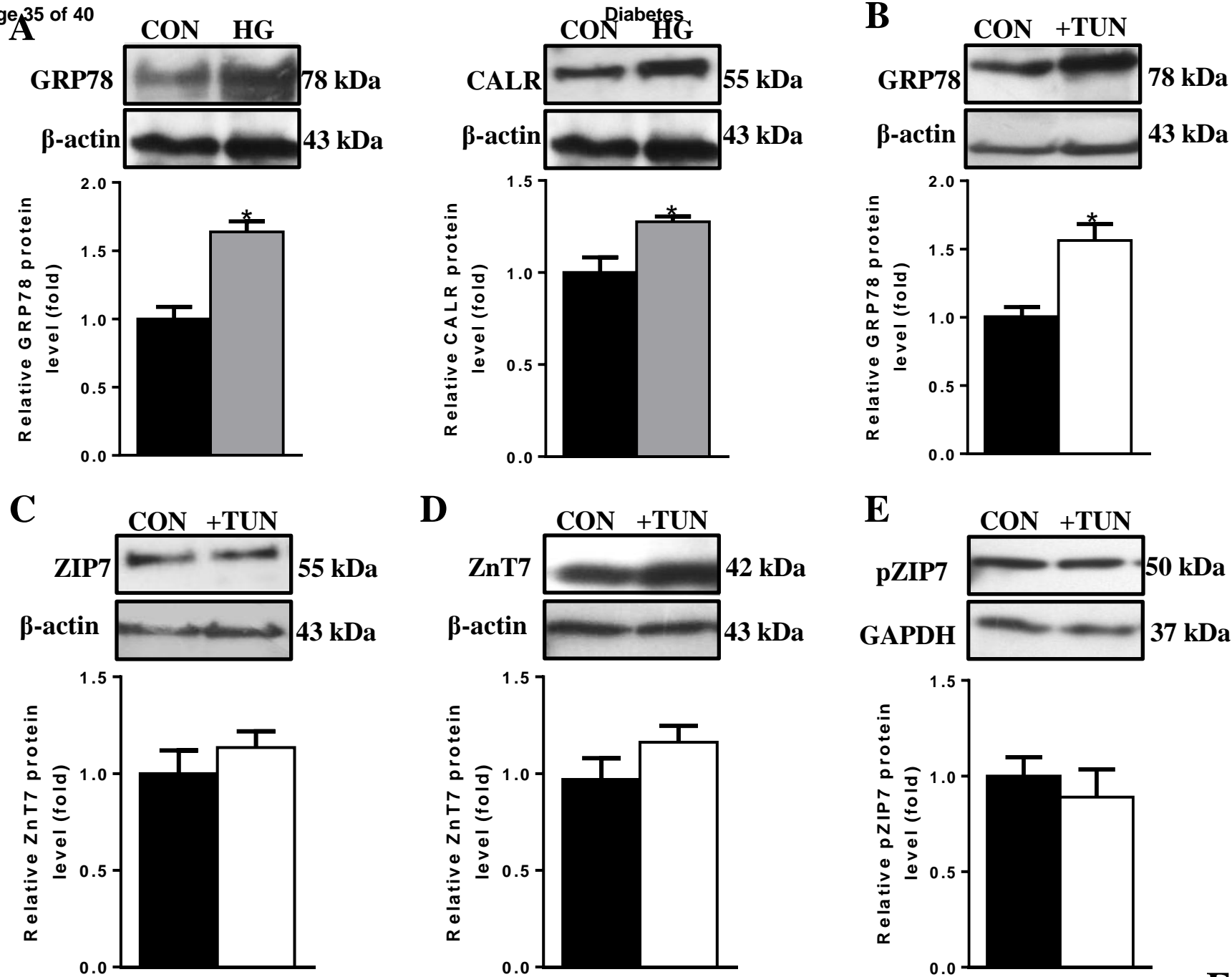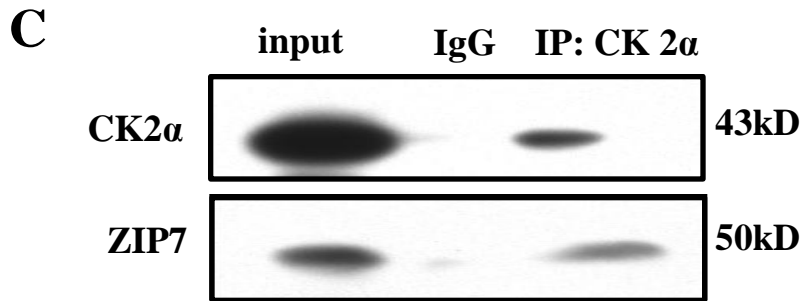
Fig.6

Fig. 7

Online Supplementary Tables

Supplementary Table 1. Effect of ZIP7-shRNA constructs upon ZIP7-expression in the cells.

	29-mer Target Sequence	29-mer ID	ZIP7/scramble
scramble	na		1.00±0.25
ZIP7-A	ACGCCTTGGAACCTCATTCGCACGATACT	HT138179A	0.65±0.18
ZIP7-B	GTGGCAACAGTGTCCGTGCTACCTGAGCT	HT138179B	0.71±0.09
ZIP7-C	GGATTCATCTATGTGGCAACAGTGTCCGT	HT138179C	0.52±0.09
ZIP7-D	GTCATGGTGACCTGCACAGAGACGTGGAA	HT138179D	0.35±0.01

**Supplementary Table 2. Sequences of primers used for qRT-PCR.**

	Sense (5`−3`)	Antisense (5`−3`)
ZIP7	CCACGGACACTCACATGAAG	CCTCTGTGGTGGAGGCTATC
ZnT7	ATGTTGCCCCTGTCCATCAAGG	TCGGAGATCAAGCCTAGGCAGT
β-actin	TGGCCTCACTGTCCACCTT	GGGCCGGACTCATCGTACT
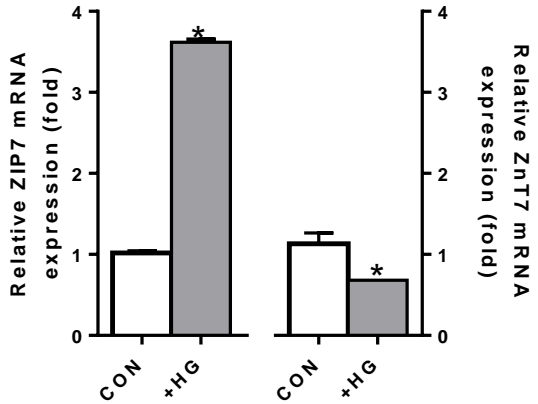
Supplementary Fig. 1:The mRNA expression levels of ZIP7 and ZnT7 in isolated cardiomyocytes from left ventricle of normal rat heart incubated with high glucose. Freshly isolated rat left ventricular cardiomyocytes incubated with high glucose (33 mM) for 3 hours (+HG group) and then examined the protein and mRNA levels of both ZIP7 and ZnT7 comparison to those of mannitol (23 mM) incubated cardiomyocytes (CON group). Bars represent mean (±SEM). Number of cells used are isolated from n=3–4 hearts/group and measurements performed with double assays in each sample from each group for each type of measurement. Significance level accepted at *p<0.05 *vs* CON.
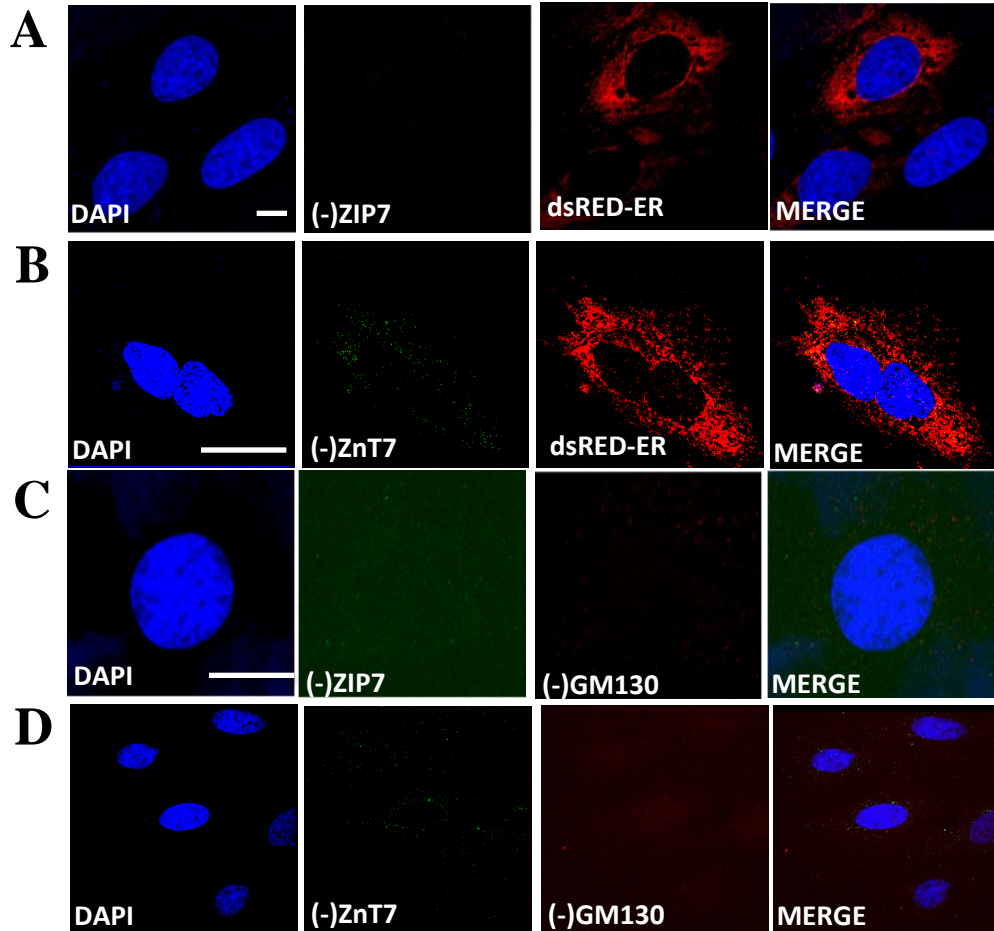
Supplementary Fig. 2. Negative controls of ZIP7, ZnT7 and GM130 in H9c2 cells. dsRED-ER(red) transfected cells were fixed and permeabilized with 4% paraformaldehyde and 0.2% Triton-X100, respectively. Cells were incubated only with secondary antibodies for ZIP7 and ZnT7 negative controls (Alexa Fluor 488 Donkey anti-Rabbit; 1:1000 and Alexa Fluor 488 Donkey anti-Goat; 1:1000, respectively) (A and B). Cells after fixation and permeabilization are incubated only with secondary antibodies for ZIP7 and GM130 negative controls (Alexa Fluor 488 Donkey anti-Rabbit; 1:1000 and Alexa Fluor 568 Goat anti-Mouse; 1:1000, respectively), secondary antibodies for ZnT7 and GM130 negative controls (Alexa Fluor 488 Donkey anti-Goat; 1:1000 and Alexa Fluor 647 Rabbit anti-Mouse; 1:1000, respectively) (C and D). They were mounted with mounting medium contains DAPI (blue).